Photoelectron spectra of the lanthanide trihalides and their interpretation[a)]

B. Ruščić,[b)] G. L. Goodman, and J. Berkowitz

Argonne National Laboratory, Argonne, Illinois 60439
(Received 8 November 1982; accepted 10 January 1983)

The He I photoelectron spectra of gaseous $LaCl_3$, $LaBr_3$, LaI_3, $CeBr_3$, CeI_3, $NdBr_3$, NdI_3, ErI_3, $LuBr_3$, and LuI_3 have been obtained. They display a pronounced increase in splitting, and hence a progressively clearer definition of peaks in the valence band as either the halogen or the lanthanide increases in atomic number. These experimental features, together with a refined relativistic $X\alpha$ DVM calculation using the von Barth–Hedin potential, have enabled us to assign these peaks with confidence. The He II photoelectron spectra of $CeBr_3$, $NdBr_3$, and LuI_3 are also presented. They reveal that the $4f$-like ionizations of early lanthanide members (e.g., Ce) occur at lower energy than the ligand valence band, but that those of late members (e.g., Lu) are corelike. The aforementioned calculations reproduce this behavior quantitatively. They also help to rationalize a bimodal behavior in the valence band; the spectra with less than half-filled $4f$ shell are very similar, as are those with more than half-filled $4f$ shell, but the two groups are distinctly different. The width of the valence bands, which varies over a factor 2.5, is correctly reproduced. The calculations have been been extended to include fluorides, where contact is made with electron impact mass spectrometry and x-ray photelectron spectra of solids, thereby enabling corrections to be made to the latter. The fragmentation behavior in mass spectrometry is then related to the states observed in photoelectron spectroscopy. Both the calculations and these experimental comparisons yield a picture in which the lanthanide fluorides display predominantly ionic bonding ($Ln^{2.2+}$); the bonding takes on succesively more covalent character as one proceeds to chlorides ($Ln^{1.6+}$), bromides ($Ln^{1.3+}$), and iodides ($Ln^{1.0+}$).

I. INTRODUCTION

In earlier work from this laboratory, we had obtained the He I photoelectron spectra[1] of several transition metal dichlorides and dibromides. These spectra were interpreted with the aid of spin-polarized $X\alpha$ calculations, from which we inferred that in early members of the $3d$ transition series (Mn, Fe) the uppermost occupied orbitals have predominantly metal $3d$ character. With increasing nuclear charge, the $3d$-like orbitals are drawn in, relative to the ligand (halogen) valence p-like orbitals. With Ni, they drop toward the bottom of the valence band. With Zn, they are distinctly corelike. There appears to be a rather pronounced change in the energy of the $3d$-like orbitals between Ni ($3d^8$) and Zn ($3d^{10}$). The low ionization energy for $3d$-like orbitals of at least the early members of the transition metal series suggests that these orbitals play a significant role in chemical bonding. These results were subsequently substantiated (more-or-less) by Lee *et al.*,[2] who obtained the He I and He II photoelectron spectra of MCl_2 (M = Cr, Mn, Fe, Co, Ni).

A natural extension of these studies was to examine the ionization energies of $4f$-like orbitals relative to ligand orbitals in the lanthanide halides. Here, according to conventional chemical wisdom, the $4f$ electrons were expected to be atomic in nature and behave largely as spectators in chemical bonding. However, some thermochemical studies on gaseous LnO and $LnCl_3$ (see Sec. V) revealed a dramatic, oscillatory variation in atomization energies across the lanthanide series, which paralleled the $4f^n \rightarrow 4f^{n-1}\,5d$ excitation energy in the atoms.

Calculational approaches to the determination of geometric and electronic structure and chemical bonding for these systems are at present very difficult. The large number of electrons precludes standard Hartree–Fock treatment; some pseudopotential technique would be required. Moreover, relativistic effects should be included. Semiempirical methods are of dubious accuracy. They require parametrization, and the necessary parameters are at best poorly known. The relativistic $X\alpha$ discrete variation method has shown some promise.[3] We have employed this method, with some significant modifications, to successfully interpret the photoelectron spectra we have obtained for the lanthanide trihalide vapors.

During the course of our investigation, a letter[4] and later a full article[5] was published by Potts and coworkers on the He I and He II photoelectron spectra of the lanthanide chlorides. In our study, we have concentrated on the lanthanide bromides and iodides. The most prominent features of these photoelectron spectra involve ionization of halogen p-like orbitals. If these features have time reversal degeneracy but are spatially nondegenerate, one can anticipate nine peaks due to ionization from these orbitals. For the chlorides, these peaks are so heavily overlapped that the spectra display two, three, or at most, four features. As we shall show below, the spectra display progressively more features as one proceeds from chlorides to bromides to iodides. As more peaks become distinguishable, it becomes possible to see the variation across the lanthanide series, a behavior very difficult to extract from the

[a)]Work supported by the U.S. D.O.E. (Office of Basic Energy Sciences) under Contract W-31-109-Eng-38.
[b)]On leave from Rugjer Bošković (Institute, Bijenička 54, P.O.B. 1016, 41001 Zagreb, Croatia, Yugoslavia.

 0021-9606/83/095443-25$2.10 © 1983 American Institute of Physics

lanthanide chloride spectra. Hence, we believe that the experimental results reported here on the lanthanide bromides and iodides provide considerably more detailed information regarding the energies of individual orbitals. This additional information has also enabled us to treat the lanthanide trihalides systematically, noting trends in bonding, adiabatic ionization potentials, and widths of valence bands. Finally, the $X\alpha$ calculational scheme which we shall describe has successfully reproduced the observations, with no adjustable shifts, and hence provides us with reliable wave functions for characterizing the properties of these molecules.

II. EXPERIMENTAL ARRANGEMENT

The hemispherical electron energy analyzer and oven system for generating high temperature vapors which we have used in these experiments were described previously.[6] A tungsten oven was used in all instances, and temperatures were measured with a chromel–alumel thermocouple. The vaporization temperature for each sample was approximately 1300 K.

Two different lamps were employed—a capillary discharge in helium, which produced almost pure He I radiation (584 Å ≡ 21.2 eV), and a hollow cathode discharge in helium, which was used to provide He II radiation (304 Å ≡ 40.8 eV).

All the samples were of commercial origin; (Mallinckrodt: $LaCl_3$; Cerac/Pure, Inc.: $LaBr_3$, LaI_3, $CeBr_3$, $NdBr_3$, NdI_3, $LuBr_3$, and LuI_3; ICN–K and K Laboratories, Inc.: CeI_3 and some of the $NdBr_3$ sample; and Alpha: ErI_3). Typically, the purity of the samples was 99.9%, except for CeI_3 and ErI_3 where it was not specified. Besides, CeI_3 was received wet, and it was necessary to dry this sample under vacuum. All other samples were anhydrous, and handled in a glove bag in a dry nitrogen atmosphere.

Samples were baked out *in situ* and monitored as the temperature increased. Evolution of H_2O, halogen gases, and hydrogen halides was observed in some of the specimens. Individual spectra were recorded on magnetic tape, and subsequently summed to improve signal to noise. Noble gases (specifically Ar and Xe) were used as calibrants for the energy scale.

III. EXPERIMENTAL RESULTS

A. He I photoelectron spectra

As mentioned earlier, we have focused our efforts on the bromides and iodides. In Fig. 1, however, we display a He I photoelectron spectrum of $LaCl_3$, partly to compare with the data of Potts and Lee,[4] and Lee *et al.*,[5] and partly to show the progressive splitting as one proceeds to the heavier halides. Our spectrum of $LaCl_3$ is very similar, in first order, to those of Refs. 4 and 5. Two broadbands are apparent. Potts and Lee[4] describe the spectrum as dividing into two regions: A low I.P. region and a high I.P. region with an intensity ratio of ~2 to 1. In our spectrum the intensity ratio is distinctly less than 2:1, and the valley between peaks is lower, indicating somewhat better resolution. There are hints of additional structure near the maximum of the high

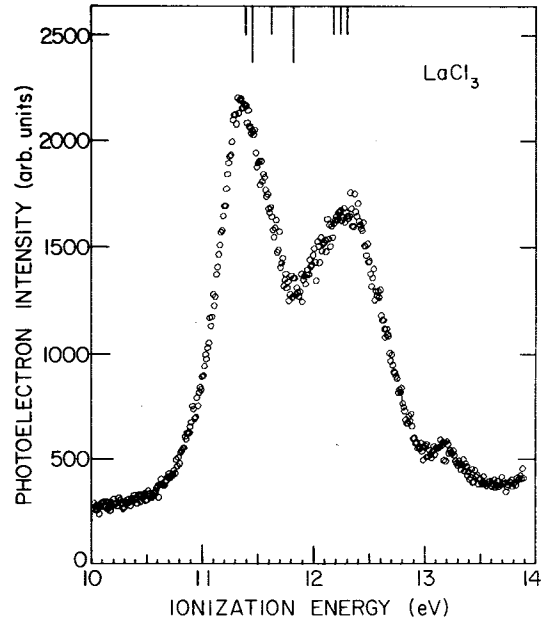

FIG. 1. The He I photoelectron spectrum of $LaCl_3$ vapor. The calculated relativistic transition state orbital energies are shown above the spectrum.

I.P. peak and to the high energy side of that peak. Lee *et al.*[5] select this latter feature, as well as the two maxima, as the only identifiable characteristics of this spectrum. We see in addition a weak peak at ~13.2 eV (Fig. 1). A peak appears at this position in the He II spectra of Refs. 4 and 5 and is attributed to ionization of helium gas by He IIδ radiation. This is extremely unlikely in our spectrum, since the capillary discharge generates almost no He IIα radiation, let alone He IIδ. The energy scales of the two sets of experiments are in reasonable concordance. Our selection of peak maxima is to higher I.P. by about 0.1 eV.

The He I spectrum of $LaBr_3$ (Fig. 2) also manifests two broad peaks, but the higher I.P. component displays at least two distinct shoulders on its high energy side. A weak peak can also be noted at ~12.65 eV. With LaI_3 (Fig. 3) the splitting becomes more apparent. Instead of two broadbands, at least five distinct peaks appear in the intense region of the spectrum, as well as a weak peak at ~12.2 eV. A characteristic diminution in adiabatic I.P. can be recognized in the sequence $LaCl_3$: $LaBr_3$: LaI_3, going from ~11.0 to ~10.0 to ~9.0 eV.

With a formal charge of +3, lanthanum would have no f electrons in these compounds. At an incident photon energy of 21.2 eV, the halogen outer p-like orbitals should be the only significant ones accessible to ionization. (In iodides, the 5s-like orbitals may be accessible, but have very low cross sections, and would appear at higher energy.) Hence, the diminution in ionization energy and the increased splitting are characteristic of the molecular orbitals formed predominantly from the halogen outer p-like orbitals. In Figs. 4–6 are shown the He I spectra of three additional bromides along the lanthanide series—$CeBr_3$, $NdBr_3$, and $LuBr_3$. In Refs. 4 and 5, the He I spectrum of $CeCl_3$ is almost identical

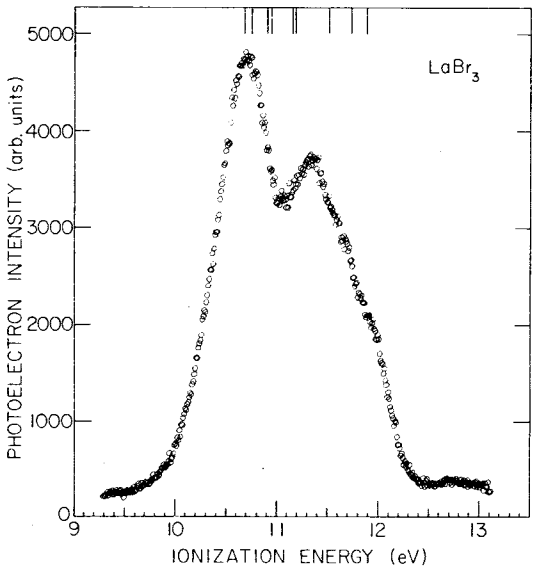

FIG. 2. The He I photoelectron spectrum of $LaBr_3$ vapor. The calculated relativistic transition state orbital energies are shown above the spectrum.

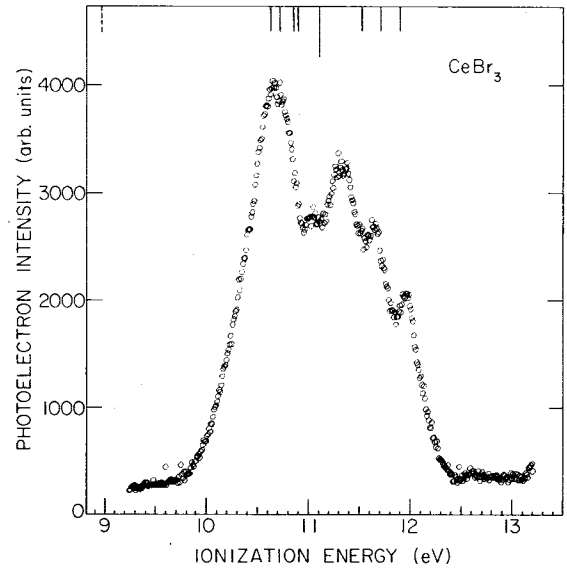

FIG. 4. The He I photoelectron spectrum of $CeBr_3$ vapor. In the calculated relativistic transition state orbital energies shown above the spectrum, the dotted line denotes a primarily f orbital.

with that of $LaCl_3$: two broadbands, with a shoulder on the high energy side of the higher I.P. band. The major difference between $CeCl_3$ and $LaCl_3$ is that the valley between the two broadbands is not as deep in $CeCl_3$. By contrast, in $CeBr_3$ (Fig. 4) four distinct peaks are readily apparent and a fifth at ~11.06 eV is highly probable. The spectrum of $NdBr_3$ (Fig. 5) is quite similar to that of $CeBr_3$. The energies of the prominent peaks appear at almost the same energy in the two spectra. The definition of peaks is not as sharp in $NdBr_3$ as in $CeBr_3$. Whether this is due to poorer resolution in the $NdBr_3$ experiment (due to deposition and contamination) or to inherently greater overlap in the spectrum is not clear at this time.

The He I spectrum of $LuBr_3$ (Fig. 6), at the end of the lanthanide series, displays still more splitting and is qualitatively different from the earlier members $CeBr_3$ and $NdBr_3$. The highest energy peak has split from the others by almost 1 eV. Six distinct peaks are observable. The He I spectrum of $LuCl_3$[4,5] also suggests this qualitative difference. The width of the valence band appears to increase from ~2.0 to ~2.5 eV across the lanthanide bromide series. The observed spectra are still primarily attributable to ionization from halogen

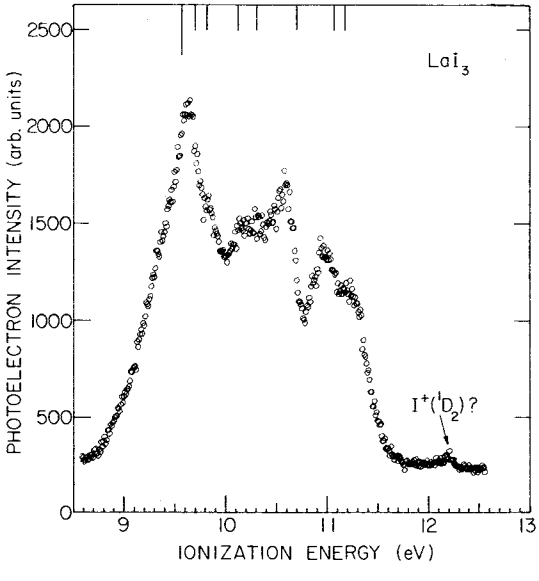

FIG. 3. The He I photoelectron spectrum of LaI_3 vapor. The calculated relativistic transition state orbital energies are shown above the spectrum.

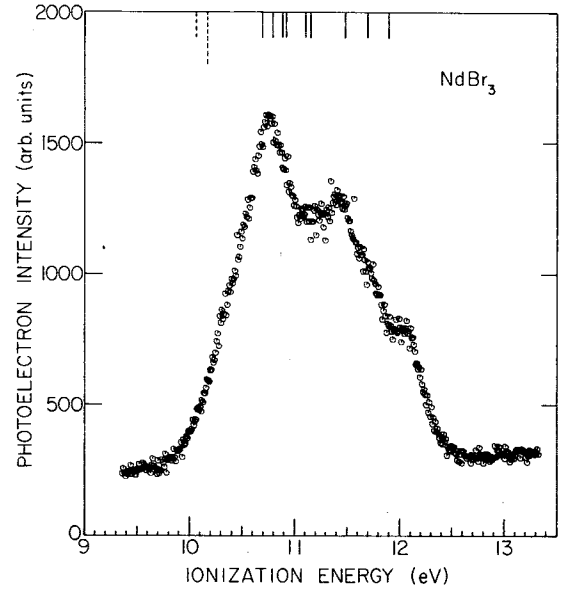

FIG. 5. The He I photoelectron spectrum of $NdBr_3$ vapor. In the calculated relativistic transition state orbital energies shown above the spectrum, the dotted lines denote primarily f orbitals.

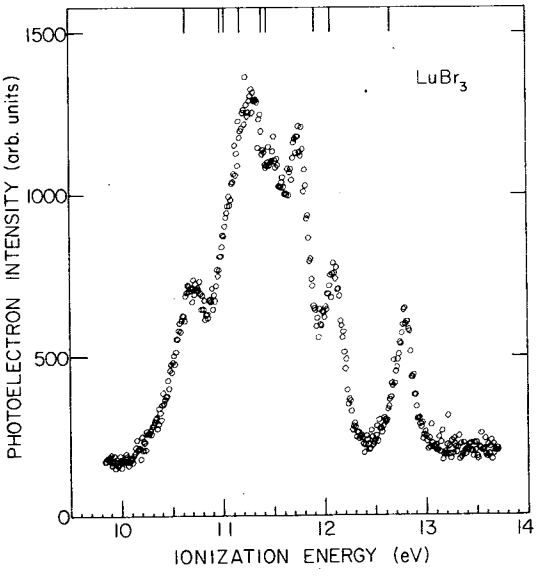

FIG. 6. The He I photoelectron spectrum of $LuBr_3$ vapor. The calculated relativistic transition state orbital energies are shown above the spectrum.

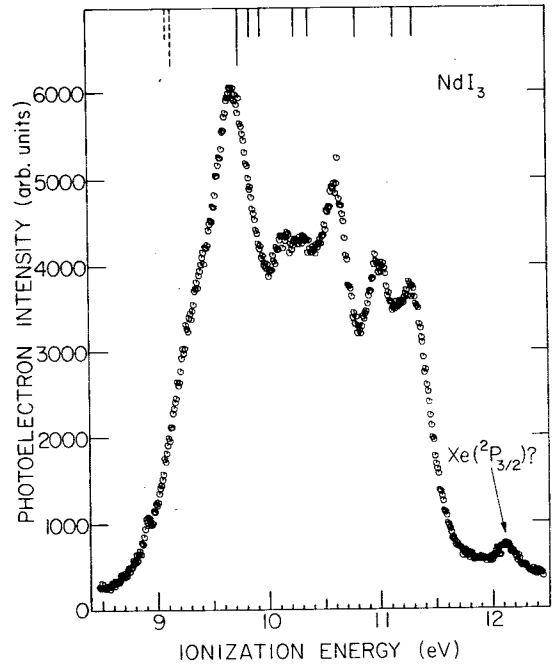

FIG. 8. The He I photoelectron spectrum of NdI_3 vapor. In the calculated relativistic transition state orbital energies shown above the spectrum, the dotted lines denote primarily f orbitals.

outer p-like orbitals, although $4f$-like orbitals may be energetically accessible, because the latter (as well as $5d$-like orbitals) generally have low ionization cross sections within a few eV of their respective thresholds. As the incident photon energy increases, the excited photoelectrons are able to surmount an angular momentum barrier and their partial cross sections for photoionization reach a maximum ~25–30 eV above their respective thresholds.

Summarizing to this point, the valence band photoelectron spectra, predominantly attributable to halogen outer p-like orbitals, display greater splitting in the sequence $LnCl_3$–$LnBr_3$–LnI_3. Across the lanthanide bromide series, the early members look very similar, and the last member reveals still more splitting, particularly the highest energy component of the valence band.

Let us now turn to the iodides. The He I spectra of CeI_3, NdI_3, ErI_3, and LuI_3 are given in Figs. 7–10, respectively. As we have learned to expect, more features are visible. Six peaks can be noted in CeI_3 and NdI_3, and as many as eight (counting shoulders) out of

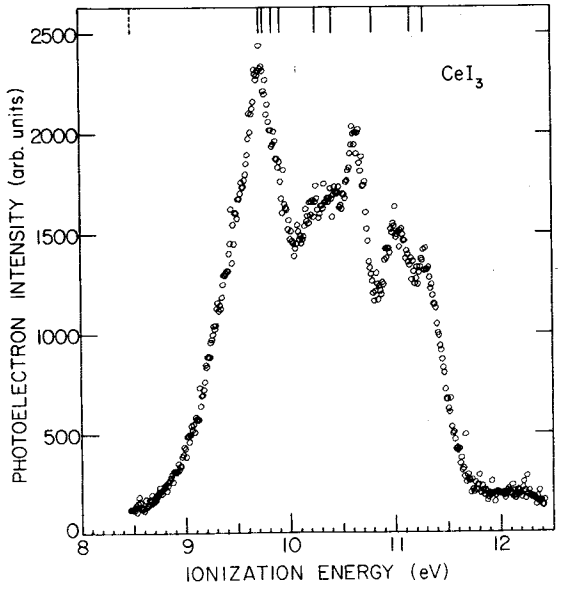

FIG. 7. The He I photoelectron spectrum of CeI_3 vapor. In the calculated relativistic transition state orbital energies shown above the spectrum, the dotted line denotes a primarily f orbital.

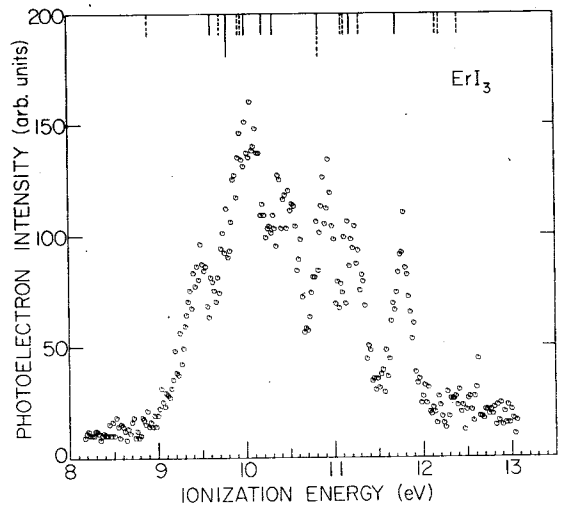

FIG. 9. The He I photoelectron spectrum of ErI_3 vapor. In the calculated relativistic transition state orbital energies shown above the spectrum, the dotted lines denote primarily f orbitals.

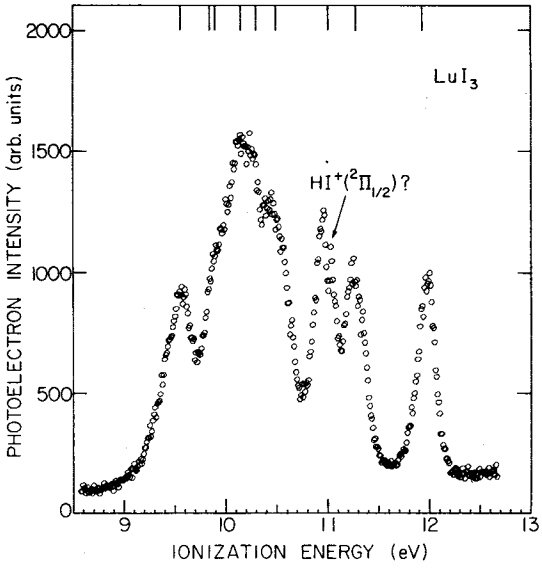

FIG. 10. The He I photoelectron spectrum of LuI_3 vapor. The calculated relativistic transition state orbital energies are shown above the spectrum.

a possible nine in LuI_3. Another striking pattern is that the spectra of CeI_3 and NdI_3 are almost identical when superimposed, as are the spectra of ErI_3 and LuI_3. The major difference in the latter two spectra is the greater splitting of the highest energy peak in LuI_3. However, the two sets are quite different from one another. We have not recorded spectra of all 15 lanthanide iodides, but from the available evidence a plausible conclusion is that the He I photoelectron spectra of those lanthanide iodides (and presumably other halides) with less than a half-filled $4f$ shell are very similar to one another, as are those with more than a half-filled $4f$ shell. To further pursue this point, we have examined the data of Ref. 5, in which 13 of the 15 lanthanide chlorides are reported. Although the definition is not as clear as with the heavier halides, it does appear as if $LaCl_3$, $CeCl_3$, $PrCl_3$, $NdCl_3$, and $SmCl_3$ display very similar He I spectra (primarily a doublet, 2:1 intensity ratio, with a shoulder on the high energy side of the higher I.P. band), whereas the spectra of $TbCl_3$, $HoCl_3$, $ErCl_3$, $TmCl_3$, $YbCl_3$, and $LuCl_3$ have in common a triplet followed by a high energy peak, the latter progressively moving to higher energy with increasing nuclear charge. The triplet has an approximate intensity ratio of 1:2:1. In $GdCl_3$, at the half-filled $4f$ shell, an intermediate behavior is observed. The initial component of the triplet is barely resolvable from the larger component, and the high energy peak is still a shoulder. We shall present our rationalization of this contrasting behavior in Sec. IV, where our calculated energies are compared with the experimental results. All of the features in the photoelectron spectra we have obtained are summarized in Table I.

B. He II photoelectron spectra

Our He II spectra were considerably weaker and more difficult to obtain, and hence we have confined our efforts to four test cases: $CeBr_3$, representing the first lanthanide having $4f$ population, $NdBr_3$ as an intermediate case, and $LuBr_3$ and LuI_3, with a completed $4f$ shell. The He II photoelectron spectra of $CeBr_3$, $NdBr_3$, and LuI_3 are shown in Figs. 11–13, respectively. In Fig. 11, a new peak appears at ~ 9.5 eV, about 1 eV lower than the first prominent peak in the He I spectrum of $CeBr_3$ (see Fig. 4). This is analogous to the observation on $CeCl_3$ reported in Refs. 4 and 5,

TABLE I. Experimental vertical ionization energies (eV).

$LaCl_3$	$LaBr_3$	LaI_3	$CeBr_3$	CeI_3
11.37	10.68	9.62	9.5[d]	9.71
11.48 (?)[e]	10.78	9.82	10.65	10.24
12.07 (?)[e]	11.04 (?)[e]	10.15	10.76 (s)[a]	10.43
12.25 (?)[e]	11.32	10.31 (?)[e]	11.05	10.60
12.35	11.65 (s)[a]	10.57	11.30[c]	10.99
13.19 (w)[b]	11.90 (s)[a]	10.92	11.64	11.28
	12.70 (w)[b]	11.21	11.97	12.2 (w)[b]
		12.16 (w)[b]	12.61 (w)[b]	
$NaBr_3$	NdI_3	ErI_3	$LuBr_3$	LuI_3
10.34 (?)[e]	8.92(?)[e]	9.52	10.71	9.57
10.74	9.4 (?)[e]	10.05	11.12 (s)[a]	9.87 (s)[a]
10.92 (s)[a]	9.69	10.27 (?)[e]	11.29	10.14
11.13	10.16	10.43	11.50	11.25 (?)[e]
11.39	10.31	10.91	11.75	10.45
11.69 (s)[a]	10.61	11.23	12.09	10.96
12.04	11.00	11.76	12.79	11.03[f]
12.9 (w)[b]	11.27		13.4 (w)[b]	11.26
	12.13 (w)[b]		16.8[d]	11.98
				16.15[d]
			18.4[d]	17.65
				18.10 (?)[d,e]

[a] Shoulder.
[b] Weak feature.
[c] Perhaps split.
[d] Observed only with He II radiation.
[e] Uncertain.
[f] Too sharp, probably $HI^+(^2\Pi_{1/2})$.

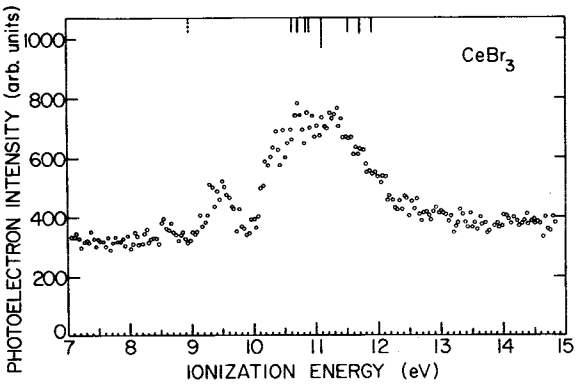

FIG. 11. The He II photoelectron spectrum of $CeBr_3$ vapor. In the calculated relativistic transition state orbital energies shown above the spectrum the dotted line denotes a primarily f orbital.

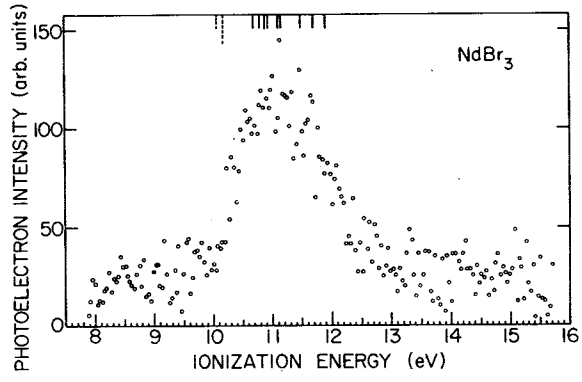

FIG. 12. The He II photoelectron spectrum of $NdBr_3$ vapor. In the calculated relativistic transition state orbital energies shown above the spectrum, the dotted lines denote primarily f orbitals.

and attributable to ionization from a $4f$-like orbital. The remainder of the spectrum, although poorly defined, yields approximately equal intensities for the lower and higher energy region of the p-like valence band, thereby emphasizing the higher energy region, relative to the He I spectrum. This is also similar to the behavior observed in $CeCl_3$, and presumably reflects some d-like character in the higher energy ionizations.

The He II spectrum of $NdBr_3$ (Fig. 12) does not reveal additional structure relative to the He I spectrum (Fig. 5) at either lower I. P. or higher I. P. This behavior also parallels that reported for $NdCl_3$.[4,5] Based on the optical absorption spectrum of aqueous Pr^{+3}[7] and intensity expressions for atomic photoelectrons,[8] we would expect the final-state multiplet splittings of the f^2 states to distribute the $4f$-like photoelectrons for the neodymium trihalides over some 0.7 eV in three prominent and three much weaker peaks. Apparently the ionization from $4f$-like orbitals for these neodymium halides is embedded in, and overlapped by the ligand valence band and is not readily distinguishable. However, a shoulder appears on the low energy side of the valence band in $NdBr_3$ (10.34 eV) which appears to be enhanced in the He II spectrum. A similar feature can be observed in NdI_3 at 9.4 eV (Fig. 8) and in the spectrum of $NdCl_3$[5] at 11.0 eV. The calculations in Sec. IV (below) indicate that the nominally f-like molecular orbitals, which are in this energy range, have a significant halogen p admixture, totaling 0.3 to 0.4 electrons. This could provide enhancement of nominally f-like features in the He I spectra. In the He II spectrum of LuI_3 (Fig. 13) two new bands appear at much higher energy (~ 16 and 17.5 eV) which were not evident in the He I spectrum (Fig. 10). With lutetium, at the end of the lanthanide series, the $4f$-like orbitals have been drawn in, and appear corelike. A similar behavior has been reported for $LuCl_3$[4,5] together with greater relative intensity of the higher energy valence bands.

Lee *et al.*[5] reported careful examination of the He II spectra of the lanthanide chlorides for $4f$-like ionization features, but could find convincing evidence only for $CeCl_3$, $NdCl_3$, and $LuCl_3$. Apparently, the inherently weaker intensity of He II spectra, possibly lower cross sections, overlapping with valence shell bands and the fine-structure splitting of the $4f$-like orbitals as the $4f$ shell fills have all combined to make these observations extremely difficult. The ionization energies from $4f$-like features in our He II spectra are also included in Table I.

In summary, the variation in ionization energy of $4f$-like transitions across the lanthanide series is akin to the variation in ionization energy of $3d$-like photoemission in the first transition metal series. Early members of the series (Ce, Pr) display $4f$-like ionizations at energies below that of the ligand valence band, intermediate ones appear to be overlapped by the valence band, and a precipitous increase in binding energy, corresponding to a corelike behavior, occurs at or near the end of the series.

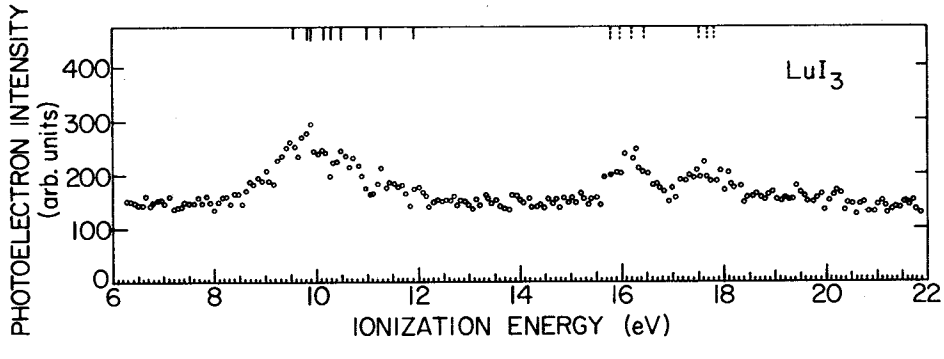

FIG. 13. The He II photoelectron spectrum of LuI_3 vapor. In the calculated relativistic transition state orbital energies shown above the spectrum, the dotted lines denote primarily f orbitals.

IV. CALCULATIONS AND ASSIGNMENTS

We are aware of four different calculations on lanthanide trihalides which are relevant to the interpretation of the vapor phase photoelectron spectra of these molecules. Myers[9] has employed a self-consistent charge, extended Hückel calculation for all of the lanthanide trihalides. His major emphasis was an attempt to distinguish between planar and pyramidal structures. His calculation was nonrelativistic, and did not include $4f$ electrons explicitly. He reported orbital energies for one species, $LaCl_3$. Invoking Koopmans' theorem, Myers' calculation yields a valence band extending from ~11.4 to ~12.7 eV, whereas the experimental values span the range ~11.4 to ~12.4 eV. In this isolated case his calculation is in surprisingly good agreement with experiment. However, it is not possible to examine trends along the lanthanide or halide series, nor is any information possible regarding the energies of the $4f$ electrons.

Pyykkö and Lohr[10] have devised a relativistically parametrized extended Hückel molecular orbital method (REX). Their major emphasis in this article was on compounds of the actinide elements. They did apply their method to lanthanide triiodides, but it was primarily directed at predicting the geometries (planar vs pyramidal) for these species. No orbital energies were reported.

Bender and Davidson[11] have performed a survey of all the lanthanide trihalides, using the Wolfsberg–Helmholz method, which is a kind of extended Hückel prescription. They have assumed planar geometry in all cases, to simplify their survey. They obtain orbital energies for the valence bands which vary with the halide, but for a particular halide they change very slightly across the lanthanide series. The span of the valence band is ~0.8, ~1.0, ~1.1, and ~1.2 eV for the fluorides, chlorides, bromides, and iodides respectively, about a factor of 2 smaller than our experimental results for the latter three. The first ionization potentials (applying Koopmans' theorem) increase from ~9.3 eV for iodides to ~12.0 eV for chlorides, somewhat more rapidly than do the experimental values (~9.0 to ~11.0 eV). Energies for the $4f$-like orbitals are also given. In fact, these authors were primarily interested in $f \leftarrow\rightarrow d$ transitions in these species as possible laser lines. We shall return to the matter of $4f$-orbital energies later. At this point, we note parenthetically that their calculation did not include spin polarization or spin-orbit splitting in the $4f$ shell.

Snow[12] has utilized a nonrelativistic multiple-scattering $X\alpha$ calculation with overlapping and nonoverlapping spheres to calculate the orbital energies of eight lanthanide chlorides and two lanthanide fluorides. He examined the effect of spin-polarized, as well as spin-restricted functions. In comparing the results of his calculations with experiment, two prominent discrepancies are apparent, both previously noted by Lee *et al.*[5]

(1) The ionization energies of the valence (halogen-like) orbitals encompass much too narrow a span, compared to experiment (~0.5 eV, compared to ~1.5–2 eV). As Lee *et al.* observe "The close proximity of these states means that these calculations cannot be taken to give a reliable orbital ordering." The center of gravity of these bands is in moderate agreement with experiment.

(2) The ionization energies for the $4f$-like orbitals in a well-defined experimental case ($LuCl_3$) were much too large (24.3–24.4 eV) compared to the experimental values of 17.39 and 18.64 eV.

None of the aforementioned calculations adequately described the span of the valence band, nor the variation in the structure of the valence band as one changed the halide or lanthanide. As a consequence, assignments of the experimental features and correlations could not be reliably undertaken. Most of the calculations were performed nonrelativisitically, and hence the splitting within the $4f$-like band could not be properly described. Hence, a more detailed, sophisticated, and relativistic version of the $X\alpha$ method, which had previously been very successful in quantitatively describing the photoelectron spectra of the silver halides,[3] was applied to the lanthanide halide problem.

The calculations that were most useful for the silver halides were fully relativistic and employed the discrete variational method (DVM) with self-consistent charge (SCC) as developed by Ellis and co-workers.[13] Observed photoelectron peaks agreed well with transition state orbital energies (TSOE's) calculated using an optimized, minimal atomic basis set (OMABS). These atomic functions are obtained by solving numerically atomic Dirac–Slater equations[14] using the orbital occupations found by a Mulliken charge analysis[15] of the occupied molecular orbitals.

In order to extend this method to the rare-earth trihalides, it was desirable to treat most of the inner shell electrons as a frozen core, to which the valence shell electrons were made orthogonal. The core orthogonalization procedure used assumes negligible overlap of distinct core orbitals. An orthogonalized valence orbital is constructed by subtracting from the original valence orbital each core orbital multiplied by its normalized overlap with that valence orbital. Comparisons of all electron and frozen-core calculations show differences of order 0.02 eV or less for the TSOE's of the valence electrons. Because some of the rare earth trihalides have just C_{3v} symmetry, the group theoretical part of the program had to be capable of correctly treating the complex conjugate pairs that are distinct irreducible representations for this type of molecular double group. In addition, moment-polarized calculations based on the two fold Krammers degeneracy were required for the open shell systems. These improvements have been reported by Ellis and Goodman.[16]

Our first $X\alpha$ calculations employed the usual Kohn–Sham (KS) exchange potential with a standard value of $\alpha = 0.7$. These calculations gave valence TSOE's that were less bound than the experimental vertical ionization potentials by about 1 eV, rather uniformly. The

TABLE II. Effects of extended basis set, potential corrector, and exchange-correlation potential for $CeBr_3$.

Symmetry assignment		f-TS -TSOE (KS Potential $\alpha = 0.7$ f-TS basis) eV	p-TS -TSOE (KS Potential $\alpha = 0.7$ f-TS basis) eV	Expt. PES eV	p-TS -TSOE (KS Potential $\alpha = 0.7$ Extended basis) eV	p-TS -TSOE (KS Pot. $\alpha = 0.7$ Ext. basis potential correct.) eV	p-TS -TSOE (VBHL potential) eV
12e1	Ce4$f_{5/2}$				6.94	7.58	
6e3		8.10[a]	6.06	9.5[b]	6.76	7.51	7.31
11e1		9.78	9.70	10.65	10.04	9.78	10.72
10e1		9.87	9.80[a]	10.76 (s)[c]	10.17[a]	9.93[a]	10.81[a]
5e3	Br4p_π	10.00	9.93		10.25	10.04	10.94
9e1		10.05	9.98	11.05	10.29	10.08	10.98
8e1		10.26	10.18		10.48	10.31	11.19
4e3		10.28	10.21	11.30	10.54	10.35	11.22
3e3		10.68	10.52	11.64	10.83	10.60	11.55
7e1	Br4p_σ	10.87	10.74		11.06	10.81	11.76
6e1		11.05	10.92	11.97	11.21	10.94	11.94
2e3		22.04	21.82		22.19	22.08	22.85
5e1	Br4$s_{1/2}$	22.21	22.06		22.41	22.26	23.07
4e1		22.52	22.46		22.80	22.57	23.45
3e1	Ce5$p_{3/2}$	25.44	24.49		24.73	25.61	25.64
1e3		25.74	24.89		25.23	25.71	26.04
2e1	Ce5$p_{1/2}$	28.13	27.06		27.44	28.18	28.25
1e1	Ce5$s_{1/2}$	43.24	41.93		42.36	43.14	43.14

[a]Transition state orbital.
[b]Observed only with He II radiation.
[c]Shoulder.

transition state orbitals divide into two distinct groups: one primarily composed of lanthanide orbitals and the other, of halogen orbitals. The TSOE's for the primarily rare earth f molecular orbital are very sensitive to whether the half-filled transition state orbital is lanthanide f or halogen p. On the other hand, the TSOE's calculated for the primarily halogen p molecular orbitals are the same to about 0.1 eV or better independent of whether the half an electron is removed from a lanthanide f or a halogen p type molecular orbital. Thus, the results reported below will in general be TSOE's for a single f-hole transition state with a corresponding f-hole atomic basis set. The TSOE's for primarily f electron orbitals were found to be very sensitive to the occupation numbers used to determine the atomic basis set. These f TSOE's when calculated self-consistently with an OMABS gave reasonable agreement with experiment for the lutetium halides, but were not bound enough for the cerium compounds.

The valence space for halogen orbitals in a minimal basis set is very fully occupied for the lanthanide trihalides. It thus seemed possible that the discrepancy between the observed and calculated valence band ionization potentials could be reduced by using an expanded basis set with additional s, p, and d halogen orbitals. The cerium halides were used for this basis set study, since they are the smallest systems with experimentally well characterized valence and f photoelectron features. The TSOE's obtained in this study for $CeBr_3$ are summarized in Table II. Column one gives the orbital symmetry labels and general atomic character for this C_{3v} molecule. Columns two and three give TSOE's for the KS exchange potential with $\alpha = 0.7$ and OMABS corre-

TABLE III. Input geometric parameters, bond distance, and X–Ln–X angle.

	La	Ce	Nd	Gd	Er	Lu
F	2.22 Å	2.18 Å	2.15 Å	2.10 Å	2.05 Å	2.02 Å
	120°	120°	120°	120°	120°	120°
Cl	2.587 Å	2.569 Å	2.545 Å	2.489 Å	2.450 Å	2.417 Å
	112.5°	111.6°	120°	120°	120°	111.5°
Br	2.741 Å	2.722 Å	2.689 Å	2.640 Å	2.594 Å	2.56 Å
	120°	115°	111°	113.8°	120°	114°
I	2.946 Å	2.927 Å	2.894 Å	2.845 Å	2.799 Å	2.766 Å
	120°	120°	120°	120°	120°	120°

TABLE IV. Lanthanum trihalides, vertical ionization energies, and relativistic transition state orbital energies (RTSOE).

Halogen	F			Cl			Br			Br			I		
Assignment	PES[b] eV	-RTSOE eV	D_{3h} MO	PES eV	-RTSOE eV	C_{3v} MO	PES eV	-RTSOE eV	C_{3v} MO	PES eV	-RTSOE eV	D_{3h} MO	PES eV	-RTSOE eV	D_{3h} MO
Xnp_π		12.52	$5e^3$	11.37	11.39	$11e1^2$	10.68	10.67	$11e1^2$	10.68	10.69	$6e5^2$		9.57	$6e5^2$
		12.58	$6e5^2$		11.44	$5e3^2$	10.78	10.76	$10e1^2$	10.78	10.77	$5e1^2$	9.62	9.58	$5e1^2$
		12.79	$5e5^2$	11.48(?)[c]	11.45	$10e1^2$		10.90	$5e3^2$		10.82	$5e3^2$		9.70	$5e3^2$
		12.98	$5e1^2$		11.62	$9e1^2$	11.04(?)[c]	10.94	$9e1^2$	11.04(?)[c]	10.89	$5e5^2$	$Ip_{3/2}$ 9.82	9.81	$5e5^2$
Xnp_z	13	13.06	$4e3^2$		11.82	$4e3^2$		11.16	$8e1^2$		11.18	$4e1^2$	10.15	10.12	$4e1^2$
		13.06	$4e1^2$		11.83	$8e1^2$		11.18	$4e3^2$	11.32	11.30	$4e3^2$	10.31(?)[c]	10.30	$4e3^2$
		13.43	$3e3^2$	12.07(?)[c]	12.18	$3e3^2$	11.32	11.51	$3e3^2$	11.65(s)[d]	11.52	$3e3^2$	10.57	10.69	$3e3^2$
Xnp_σ		13.44[a]	$3e1^{1.5}$	12.25(?)[c]	12.24[a]	$7e1^{1.5}$	11.65(s)[d]	11.73[a]	$7e1^{1.5}$		11.83[a]	$4e5^{1.5}$	$Ip_{1/2}$ 10.92	11.07[a]	$4e5^{1.5}$
		13.46	$4e5^2$	12.35	12.30	$6e1^2$	11.90(s)[d]	11.89	$6e1^2$	11.90(s)[d]	11.95	$3e1^2$	11.21	11.17	$3e1^2$
		31.27	$2e1^2$		22.77	$2e3^2$		22.66	$2e3^2$		22.66	$2e3^2$		20.15	$2e3^2$
Xns	34	31.83	$1e3^2$		23.06	$5e1^2$		22.91	$5e1^2$		22.93	$3e5^2$		20.26	$3e5^2$
		31.93	$1e5^2$		23.64	$4e1^2$		23.39	$4e1^2$		23.50	$2e1^2$		20.54	$2e1^2$
		24.26	$2e3^2$		25.43	$3e1^2$		25.00	$3e1^2$		24.98	$2e5^2$		24.38	$2e5^2$
La 5p	22	24.62	$3e5^2$		26.01	$1e3^2$		25.55	$1e3^2$		25.65	$1e3^2$		24.72	$1e3^2$
	25	26.88	$2e5^2$		27.76	$2e1^2$		27.41	$2e1^2$		27.49	$1e5^2$		26.92	$1e5^2$
La 5s		41.94	$1e1^2$		41.91	$1e1^2$		41.64	$1e1^2$		41.71	$1e1^2$		41.92	$1e1^2$

Lanthanum trihalides, SCC orbital occupations, and basis set ionicities.

Orbital	F ρ	Cl ρ	Br ρ	I ρ
$4f_{5/2}$	0.087	0.076	0.077	0.087
$4f_{7/2}$	0.111	0.098	0.087	0.091
$5s_{1/2}$	1.998	1.997	2.000	2.007
$5p_{1/2}$	1.997	1.997	1.998	2.001
$5p_{3/2}$	3.991	3.990	3.993	3.997
$5d_{3/2}$	0.320	0.514	0.551	0.634
$5d_{5/2}$	0.462	0.648	0.707	0.743
$6s_{1/2}$	0.009	0.054	0.094	0.165
$6p_{1/2}$	0.009	0.024	0.035	0.070
$6p_{3/2}$	0.008	0.026	0.044	0.105
Q (La)	2.007	1.574	1.413	1.098
$ns_{1/2}$	1.987	1.984	1.993	1.991
$np_{1/2}$	1.835	1.809	1.759	1.707
$np_{3/2}$	3.680	3.564	3.552	3.501
Q(X)	−0.502	−0.358	−0.304	−0.199
Q_{BASIS} (La)	1.865	1.518	1.425	1.071
Q_{BASIS} (X)	−0.454	−0.340	−0.308	−0.189

[a]Transition state orbital. [b]Reference 23. [c]Uncertain. [d]Shoulder.

TABLE V. Cerium trihalides, vertical ionization energies, and transition state orbital energies (TSOE).

Halogen	F			Cl						Br			I		
Assignment	PES[a] eV	RDVM -TSOE eV	D_{3h} MO	PES[b] eV	RDVM -TSOE eV	C_{3v} MO	DVM -TSOE eV	C_{3v} MO	MS$X\alpha$[c] -TSOE eV	PES eV	RDVM -TSOE eV	C_{3v} MO	PES eV	RDVM -TSOE eV	D_{3h} MO
Ce5$f_{5/2}\alpha$	8	10.14[d]	7e5	9.82	9.48[d]	12e1	9.15[d]	6e	10.6	9.5[f]	8.98[d]	12e1		8.50[d]	6e3
		12.84	5e3	11.33	11.47	11e1	11.46	5e	11.7	10.65	10.63	11e1	9.71	9.73	6e5
		12.90	6e5		11.52	5e3				10.76(s)[g]	10.72	10e1		9.76	5e1
		13.06	5e5	11.58	11.54	10e1	11.53	$1a_2$	12.0		10.85	5e3		9.85	5e3
Xnp_π		13.30	5e1		11.72	9e1	11.65	$5a_1$	11.9		10.89	9e1		9.93	5e5
	13	13.35	4e3		11.92	4e3				11.05	11.11	8e1	I5$p_{3/2}$ 10.24	10.26	4e1
							11.88	4e	12.0						
		13.36	4e1		11.93	8e1					11.12	4e3	10.43	10.42	4e3
		13.76	3e3	12.25	12.35	3e3				11.30[e]	11.52	3e3	10.60	10.80	3e3
Xnp_σ		13.79	4e5		12.39	7e1	12.12	$4a_1$	12.1	11.64	11.71	7e1	I5$p_{1/2}$ 10.99	11.16	4e5
		13.83	3e1	12.60	12.45	6e1	12.17	3e	12.1	11.97	11.89	6e1	11.28	11.28	3e1
		31.58	2e1		23.24	2e3					22.84	2e3		20.34	2e3
Xns	34	32.29	1e3				22.45	2e	23.2						
					23.43	5e1					23.00	5e1		20.43	3e5
		32.55	1e5		23.79	4e1	23.12	$3a_1$	23.5		23.31	4e1		20.65	2e1
		26.05	2e3		26.90	3e1	24.57	$2a_1$	26.1		26.32	3e1		25.50	2e5
Ce5$p_{3/2}$	24				27.28	1e3					26.61	1e3		25.81	1e3
		26.51	3e5				25.50	1e	26.5						
Ce5$p_{1/2}$	27	28.94	2e5		29.59	2e1					29.02	2e1		28.31	1e5
Ce5$s_{1/2}$		45.08	1e1		44.70	1e1	37.80	$1a_1$	40.6		44.13	1e1		43.49	1e1

Cerium trihalides, SCC orbital occupations, and basis set ionicities.

	F		Cl-REL		Cl-NRL		Br		I	
Orbital	ρ	σ	ρ	σ	ρ	σ	ρ	σ	ρ	σ
$4f_{5/2}$	0.7267	0.4982	0.6546	0.4822			0.7414	0.0	0.7758	0.0
					1.3283	0.6466				
$4f_{7/2}$	0.2950	0.0246	0.2432	0.0536			0.2453	0.0	0.2478	0.0
$5s_{1/2}$	1.9990	−0.0001	1.9987	−0.0003	1.9984	−0.0003	1.9982	0.0	2.0025	0.0
$5p_{1/2}$	1.9960	0.0001	1.9987	−0.0001			1.9979	0.0	2.0014	0.0
					5.9895	−0.0011				
$5p_{3/2}$	3.9862	−0.0006	3.9937	−0.0008			3.9937	0.0	4.0018	0.0
$5d_{3/2}$	0.3611	0.0047	0.5269	0.0062			0.6034	0.0	0.6467	0.0
					1.1496	0.0095				
$5d_{5/2}$	0.5120	0.0083	0.7435	0.0087			0.8168	0.0	0.8287	0.0
$6s_{1/2}$	0.0068	0.0004	0.0772	0.0013	0.0350	−0.0000	0.1255	0.0	0.1911	0.0
$6p_{1/2}$	0.0059	0.0012	0.0329	0.0012			0.0508	0.0	0.0808	0.0
					0.0467	0.0010				
$6p_{3/2}$	0.0007	0.0008	0.0391	0.0011			0.0699	0.0	0.1208	0.0

TABLE V (*Continued*)

Orbital	F		Cl-REL		Cl-NRL		Br		I	
	ρ	σ	ρ	σ	ρ	σ	ρ	σ	ρ	σ
Q(Ce)	2.111		1.691		1.452		1.358		1.103	
$ns_{1/2}$	1.9907	−0.0001	1.9903	−0.0001	1.9885	−0.0002	1.9950	0.0	1.9931	0.0
$np_{1/2}$	1.8523	−0.0051	1.8245	−0.0052			1.8121	0.0	1.8138	0.0
					5.3290	−0.0517				
$np_{3/2}$	3.6939	−0.0074	3.5824	−0.0124			3.4793	0.0	3.3940	0.0
Q(X)	−0.537		−0.397		−0.318		−0.286		−0.201	
Q_{BASIS} (Ce)	2.011		1.826		1.660		1.374		1.231	
Q_{BASIS} (X)	−0.5035		−0.442		−0.387		−0.301		−0.238	

[a]Reference 23.
[b]Reference 5.
[c]Reference 12.
[d]Transition state orbital.
[e]Perhaps split.
[f]He II radiation only.
[g]Shoulder.

sponding to an f electron transition state and to a p electron transition state, respectively. The sensitivity of the primarily f electron ionization potential shifting from 8.10 to 6.06 eV and the relative insensitivity of the valence band, primarily halogen p ionization potentials, which span ~ 9.8 to ~11.0 eV in both cases, are well illustrated here. Both of these sets of calculated ionization potentials for the halogen orbitals are about 1 to 1.8 eV less bound than the experimental results given in column four.

Column five lists TSOE's for the extended basis set with $5s_{1/2}$, $5p_{1/2}$, and $5p_{3/2}$ added to the atomic bromine basis functions. Although the agreement with observations seems slightly better, there is still a discrepancy of 0.5 to 0.75 eV for the valence band. According to Mulliken analysis of the occupied orbitals only 0.001, 0.01, and 0.02 electrons are in the $5s_{1/2}$, $5p_{1/2}$, and $5p_{3/2}$ orbitals, respectively—quite small amounts. Delley and Ellis[17] have emphasized the close relation between basis set size and adequacy of representation of the molecular electrostatic potential energy. Thus, we have also applied a multipole expansion technique developed by these authors to correct for inadequacies of the SCC potential. For $CeBr_3$, as shown in column six of Table II, the combined influence of an expanded basis set together with a potential corrector using both monopole and dipole terms for all atoms is to produce just about the same TSOE's as those in columns two or three from OMABS and in the SCC approximation. Thus, it appears that the TSOE's for valence electrons of the lanthanide trihalides are indeed highly sensitive to the details of the molecular potential function. But there seem to be some other physical effects not yet taken into account.

At the suggestion of Professor D. E. Ellis, we tried replacing the standard KS exchange potential with the exchange-correlation potential developed by Hedin and Lundqvist,[18] extended to the spin polarized case by von Barth and Hedin,[19] and generalized to fully relativistic moment-polarized calculations by Ellis and Goodman.[16] This von Barth–Hedin–Lundqvist (VBHL) potential is particularly sensitive to the diffuseness of electron orbitals, yielding more binding than the KS potential for very diffuse orbitals and less binding for corelike orbitals.

The VBHL potential with an OMABS for $CeBr_3$ yielded TSOE's that agree quite well with the observed photoelectron spectrum. Column seven of Table II gives the p-TSOE's for a OMABS in the SCC approximation for $CeBr_3$. Similar shifts from the KS exchange potential results were also observed for the VBHL exchange-correlation potential with other rare earth trihalides. In each case the VBHL results agree well with experimental photoelectron spectra, both in overall width and in absolute binding energy.

Using the VBHL potential, DVM-SCC relativistic, transition state ionization potentials with OMABS have been calculated for 24 rare earth trihalides: fluorides, chlorides, bromides, and iodides of lanthanum, cerium, neodymium, gadolinium, erbium, and lutetium. Five

TABLE VI. Neodymium trihalides, vertical ionization energies, and transition state orbital energies (TSOE).

Halogen		F			Cl			Br				I		
Assignment	PES[a] eV	RDVM -TSOE eV	D_{3h} MO	PES[b] eV	RDVM -TSOE eV	D_{3h} MO	PES eV	RDVM -TSOE eV	C_{3v} MO		PES eV	RDVM -TSOE eV	D_{3h} MO
		11.37	6e1	(11.0)	10.80	6e1		10.07	13e1		8.92(?)[d]	9.10	6e1
Nd4$f_{5/2}$α	10	11.57	6e3	12	10.75	7e5	10.34(?)[d]	10.18	12e1			9.14	7e5
		11.58[c]	7e5		10.68[c]	6e3		10.18[c]	6e3		9.4(?)[d]	9.14[c]	6e3
				11.16									
		13.03	5e3	11.47	11.51	6e5		10.69	11e1			9.74	6e5
							10.74						
		13.06	6e5		11.52	5e3		10.80	10e1			9.75	5e1
											9.69		
		13.21	5e5		11.58	5e1		10.89	5e3	15$p_{3/2}$		9.85	5e3
							10.92(s)[e]						
Xnp_π	13	13.42	5e1		11.68	5e5		10.93	9e1			9.94	5e5
		13.47	4e3		11.90	4e1		11.12	8e1		10.16	10.24	4e1
							11.13						
		13.49	4e1		11.91	4e3		11.16	4e3		10.31	10.37	4e3
		13.88	3e3	12.28	12.32	3e3	11.39	11.48	3e3		10.61	10.79	3e3
Xnp_σ		13.91	4e5		12.39	4e5	11.69(s)[e]	11.70	7e1	15$p_{1/2}$	11.00	11.13	4e5
		13.99	3e1	12.74	12.68	3e1	12.04	11.90	6e1		11.27	11.30	3e1
		31.74	2e1		23.29	2e3		22.94	2e3			20.37	2e3
Xn s	34												
		32.56	1e3		23.49	3e5		23.09	5e1			20.45	3e5
		33.09	1e5		23.93	2e1		23.35	4e1			20.66	2e1
		26.90	2e3		27.59	2e5		27.14	3e1			26.17	2e5
Nd5$p_{3/2}$	24												
		27.67	3e5		28.07	1e3		27.22	1e3			26.46	1e3
Nd5$p_{1/2}$	28	30.17	2e5		30.83	1e5		30.07	2e1			28.89	1e5
Nd5$s_{1/2}$		47.84	1e1		47.19	1e1		46.39	1e1			45.72	1e1

Neodymium trihalides, SCC orbital occupations, and basis set ionicities.

	F		Cl		Br		I	
Orbital	ρ	σ	ρ	σ	ρ	σ	ρ	σ
$4f_{5/2}$	2.5337	2.3563	2.6084	2.4643	2.6338	2.4781	2.6055	2.5159
$4f_{7/2}$	0.5182	0.3183	0.4392	0.2842	0.4472	0.3971	0.5268	0.3926
$5s_{1/2}$	1.9996	−0.0006	2.0021	−0.0009	2.0012	−0.0010	2.0035	−0.0009
$5p_{1/2}$	1.9973	−0.0006	1.9987	−0.0007	2.0033	−0.0005	2.0029	−0.0006
$5p_{3/2}$	3.9886	−0.0027	3.9944	−0.0022	4.0034	−0.0024	4.0051	−0.0015
$5d_{3/2}$	0.3578	0.0238	0.4991	0.0284	0.5579	0.0344	0.5948	0.0306
$5d_{5/2}$	0.4938	0.0222	0.6962	0.0338	0.7516	0.0382	0.7620	0.0328
$6s_{1/2}$	0.0118	0.0040	0.0931	0.0121	0.1531	0.0155	0.2133	0.0120
$6p_{1/2}$	0.0059	0.0023	0.0474	0.0056	0.0583	0.0047	0.0984	0.0060
$6p_{3/2}$	−0.0012	0.0034	0.0558	0.0036	0.0728	0.0032	0.1354	0.0024
Q(Nd)	2.095		1.566		1.317		1.052	
$ns_{1/2}$	1.9925	−0.0004	1.9908	−0.0004	1.9936	−0.0002	1.9894	−0.0002
$np_{1/2}$	1.8419	−0.0342	1.7890	−0.0455	1.8088	−0.0416	1.8202	−0.0186
$np_{3/2}$	3.6971	−0.0410	3.5754	−0.0634	3.4705	−0.1140	3.3744	−0.1031
Q(X)	−0.532		−0.355		−0.273		−0.184	
Q_{BASIS}(Nd)	1.992		1.560		1.347		1.118	
Q_{BASIS}(X)	−0.498		−0.353		−0.282		−0.206	

[a]Reference 23.
[b]Reference 5. [Value in parenthesis is recognizable in Fig. 2(b) but not recorded in Tables 1 and 2].
[c]Transition state orbital.
[d]Uncertain.
[e]Shoulder.

compounds have also been studied nonrelativistically within these approximations: cerium trichloride and the four lutetium trihalides. The relativistic and nonrelativistic calculations differ in the atomic basis functions and the kinetic energy for the molecular problem. Otherwise, they use essentially the same procedures. Experimental bond distances and angles were used when known.[20] In other cases estimated bond distances for a planar geometry were used. These input parameters are summarized in Table III. Atomic orbital basis functions were calculated in a potential well of radius 8 a.u. and depth 1 Ry to further localize diffuse valence orbitals. The number of points for the discrete variational grid was typically 1500–1800, 1200–2100, 3000–3300, or 2100–4500 for fluorides, chlorides, bromides, or iodides, respectively.

Tables IV through IX list observed vertical ionization energies, assigning them to calculated TSOE's with molecular orbital designations and gross atomic orbital assignments for the trihalides of lanthanum, cerium, neodymium, gadolinium, erbium, and lutetium, re-

TABLE VII. Gadolinium trihalides, vertical ionization energies, and transition state orbital energies (TSOE).

Halogen	F			Cl			Br			I		
Assignment	PES[a] eV	RDVM -TSOE eV	D_{3h} MO	PES[b] eV	RDVM -TSOE eV	D_{3h} MO	RDVM -TSOE eV	C_{3v} MO		RDVM -TSOE eV	D_{3h} MO
Xnp_π		12.77	7e3	11.36	11.56	8e1	10.72	16e1		9.76	8e1
		12.81	8e5	11.69	11.70	8e5	10.94	15e1		9.91	8e5
		12.89	8e1		11.71	7e3	11.00	7e3		9.99	7e3
									I5$p_{3/2}$		
		12.93	7e5		11.82	7e5	11.14	14e1		10.14	7e5
		13.22	7e1	12.14	12.04	7e1	11.26	13e1		10.40	7e1
		13.22	6e3		12.04	6e3	11.33	6e3		10.57	6e3
Xnp_σ		13.73	6e1	12.37	12.56	5e3	11.72	5e3		11.03	5e3
		13.77	5e3		12.63	6e5	11.89	12e1	I5$p_{1/2}$	11.36	6e5
		13.80	6e5	12.87	12.89	6e1	12.18	11e1		11.64	6e1
Gd4$f_{7/2}{}^\alpha$		15.16	4e3	15.5	14.51	5e1	13.93	4e3		12.91	5e5
		15.18	5e1		14.54	5e5	13.94	10e1		13.02	4e3
		15.24	5e5		14.56	4e3	13.97	9e1		13.09[c]	5e1
	15	15.26	4e1		14.66	4e1	14.00	8e1		13.23	4e1
		15.93[c]	3e3		15.31	4e5	14.70	7e1		13.75	3e3
Gd4$f_{5/2}{}^\alpha$		15.94	3e1		15.34[c]	3e3	14.73	6e1		13.80	4e5
		15.98	4e5	16.5	15.39	3e1	14.74[c]	3e3		13.94	3e1
Gd5p	28	29.18	2e3		23.74	2e3	23.32	2e3		20.68	2e3
		29.86	3e5		23.87	3e5	23.40	5e1		20.74	3e5
	32	31.58	2e1		24.16	2e1	23.58	4e1		20.92	2e1
Xns		32.20	2e5		30.81	2e5	29.71	3e1		29.60	2e5
	34	33.24	1e3		31.11	1e3	29.89	1e3		29.81	1e3
		35.83	1e5		35.16	1e5	34.52	2e1		33.94	1e5
Gd5s		54.61	1e1		54.25	1e1	53.58	1e1		53.40	1e1

Gadolinium trihalides, SCC orbital occupations and basis set ionicities

Orbital	F		Cl		Br		I	
	ρ	σ	ρ	σ	ρ	σ	ρ	σ
$4f_{7/2}$	2.6617	2.3564	2.6835	2.3203	2.7083	2.2975	3.0427	2.9308
$4f_{5/2}$	4.1194	3.8716	4.1074	3.8891	4.0918	3.9078	3.7152	3.6359
$5s_{1/2}$	1.9998	−0.0007	2.0031	−0.0014	2.0026	−0.0018	2.0087	−0.0022
$5p_{1/2}$	2.0002	−0.0007	1.9998	−0.0008	2.0033	−0.0011	2.0031	−0.0020
$5p_{3/2}$	3.9973	−0.0011	3.9982	−0.0017	4.0060	−0.0021	4.0053	−0.0035
$5d_{3/2}$	0.4363	0.0435	0.5412	0.0605	0.5960	0.0783	0.6185	0.0944
$5d_{5/2}$	0.6092	0.0557	0.7497	0.0762	0.7942	0.0944	0.7857	0.1118
$6s_{1/2}$	0.0492	0.0121	0.1454	0.0224	0.2311	0.0302	0.3312	0.0355
$6p_{1/2}$	0.0273	0.0037	0.0697	0.0096	0.0842	0.0087	0.1441	0.0156
$6p_{3/2}$	0.0322	0.0051	0.0952	0.0143	0.1136	0.0136	0.2048	0.0246
Q(Ga)	2.067		1.609		1.369			1.141
$ns_{1/2}$	1.9836	0.0001	1.9923	0.0003	1.9947	0.0002	1.9899	−0.0002
$np_{1/2}$	1.8554	0.0136	1.8091	0.0061	1.8161	0.0016	1.8085	−0.0259
$np_{3/2}$	3.6835	0.0377	3.5684	0.0295	3.4787	0.0158	3.4158	−0.0789
Q(X)	−0.522		−0.370		−0.2896			−0.214
Q_{BASIS} (Ga)	1.759		1.605		1.442			1.332
Q_{BASIS} (X)	−0.422		−0.368		−0.314			−0.279

[a]Reference 23. [b]Reference 5. [c]Transition state orbital.

spectively. The results for lanthanum and cerium are given for moment-restricted calculations in which both moment-up and moment-down electrons see the same average exchange-correlation field. Since the net moment polarization in these cases is of order 1/2, spin polarization splittings are only 0.1 to 0.2 eV.

For the rare earth compounds with more than one f electron moment-polarization effects become significant for the primarily f electrons—of order 0.5 eV—although they remain small for the primarily halogen p electrons. Thus, in Tables VI through IX the results of moment-polarized transition state calculations are reported in an abbreviated fashion: the average of moment-up and moment-down orbital energies is given for the orbitals other than rare earth f orbitals, while

TABLE VIII. Erbium trihalides-vertical ionization energies and relativistic transition state orbital energies (RTSOE).

Halogen	F			Cl				Br			I			
Assignment	PES[a] eV	-RTSOE eV	D_{3h} MO	PES[b] eV	-RTSOE eV	D_{3h} MO	Assign.	-RTSOE eV	D_{3h} MO	Assign.	PES eV	-RTSOE eV	D_{3h} MO	Assign.
Er$4f_{7/2}\beta$		12.76[d]	10e5		10.90[d]	9e3	$4f_{7/2}\beta$	10.46[d]	10e1	$4f_{7/2}\beta$		8.91[d]	10e1	$4f_{7/2}\beta$
	12	13.50	9e1											
Er$4f_{5/2}\beta$		13.68	9e5	11.54	11.59	9e1		10.91	9e1		9.52	9.62	9e1	I$5p_{3/2}$
		13.73	8e3		11.82	9e5		11.05	9e5			9.72	9e5	$4f_{5/2}\beta$
					11.83	8e3	C1$3p_\pi$	11.09	8e3	Br$4p_\pi$		9.80	8e5	
		14.04	8e5	11.90	11.92	8e5		11.18	8e5					I$5p_{3/2}$
F$2p_\pi$		14.04	7e3		12.08	7e3		11.33	8e1			9.81	8e3	
		14.08	8e1	12.13	12.09	8e1		11.50	7e3			9.93	7e3	$4f_{5/2}\beta$
												9.96	8e1	
		14.27	7e5		12.22	7e5		11.66	7e5		10.05	10.00	7e5	
		14.43	6e3		12.22	7e1	$f_{5/2}\beta$	11.68	6e3	$f_{5/2}\beta$	10.27(?)[f]	10.20	7e1	I$5p_{3/2}$
		14.44	7e1	12.41[e]	12.26	6e3		11.69	7e1		10.43	10.32	6e3	
Er$f_{7/2}\alpha$		14.70	5e3	12.58	12.60	5e3	C1$3p_\sigma$	11.80	5e3			10.83	6e5	$4f_{7/2}\alpha$
F$2p_\sigma$+Er$(4f_{7/2}+4f_{5/2})$		14.73	6e1	12.60[e]	12.66	6e1	$f_{7/2}\alpha$	12.08	6e5	Br$4p_\sigma$	10.91	10.84	5e3	I$5p_{1/2}$
Er$4f_{7/2}\alpha$		14.75	6e5		12.68	6e5	C1$3p_\sigma$	12.44	6e1					
(Er$4f_{7/2}$+F$2p_\sigma$)α		14.90	5e1									11.09	6e1	
					12.83	5e1		12.56	4e3			11.12[e]	4e3	$4f_{7/2}\alpha$
F$2p_\sigma$		15.00	4e3		12.92	5e5	$4f_{7/2}\alpha$	12.59	5e5	$4f_{7/2}\alpha$	11.23	11.18	5e5	I$5p_{1/2}$
		15.04	5e5		12.92	4e3		12.60	5e1			11.29	5e1	$4f_{7/2}\alpha$
				13.17	13.72	4e1	C1$3p_\sigma$	12.82	4e1		11.76	11.70	4e1	I$5p_{1/2}$
Er$(4f_{7/2}+4f_{5/2})\alpha$+F$2p_\sigma\alpha$		15.32	4e1											
		15.88	3e3	15–16	13.99	4e5		13.69	4e5			12.15	4e5	
Er$4f_{5/2}\alpha$	15	15.91[c]	4e5		14.00	3e3	$4f_{5/2}\alpha$	13.71	3e3	$4f_{5/2}\alpha$		12.19	3e3	$4f_{5/2}\alpha$
		15.99	3e1		14.10[c]	3e1		13.71[c]	3e1			12.40	3e1	
Er$5p_{3/2}$+F$2s_{1/2}$		31.35	2e3		23.97	2e3		23.52	2e3			20.50	2e3	
F$2s_{1/2}$		32.00	3e5		24.09	3e5	C1$3s_{1/2}$	23.60	3e5	Br$4s_{1/2}$		20.56	3e5	I$5s_{1/2}$
	34	33.00	2e1		24.36	2e1		23.80	2e1			20.74	2e1	
Er$5p_{3/2}$		34.61	2e5		32.70	2e5	Er$5p_{3/2}$	32.41	2e5	Er$5p_{3/2}$		31.17	2e5	
Er$5p_{3/2}$+F$2s_{1/2}$		35.39	1e3		32.96	1e3		32.61	1e3			31.35	1e3	Er$5p_{3/2}$
Er$5p_{1/2}$	37	39.84	1e5		38.33	1e5	Er$5p_{1/2}$	38.03	1e5	Er$5p_{1/2}$		36.78	1e5	Er$5p_{1/2}$
Er$5s_{1/2}$		61.56	1e1		60.13	1e1	Er$5s_{1/2}$	59.81	1e1	Er$5s_{1/2}$		58.52	1e1	Er$5s_{1/2}$

Erbium trihalides, SCC orbital occupations and basis set ionicities.

	F		Cl		Br		I	
Orbital	ρ	σ	ρ	σ	ρ	σ	ρ	σ
$4f_{5/2}$	5.4991	−0.4229	5.7285	−0.4648	5.6514	−0.3232	5.8718	−0.1005
$4f_{7/2}$	5.2888	2.6952	5.2393	2.6943	5.3063	2.6802	5.2039	2.4635
$5s_{1/2}$	2.0004	−0.0002	2.0010	−0.0001	2.0017	−0.0009	2.0065	−0.0005
$5p_{1/2}$	2.0016	−0.0004	1.9996	−0.0001	2.0039	−0.0008	2.0026	−0.0015
$5p_{3/2}$	4.0002	0.0014	3.9986	−0.0003	4.0073	−0.0005	4.0040	−0.0025
$5d_{3/2}$	0.3555	0.0100	0.4733	0.0189	0.5034	0.0178	0.5145	0.0214

TABLE VIII (*Continued*)

Erbium trihalides, SCC orbital occupations and basis set ionicities.

	F		Cl		Br		I	
Orbital	ρ	σ	ρ	σ	ρ	σ	ρ	σ
$5d_{5/2}$	0.4888	0.0137	0.6562	0.0249	0.6740	0.0225	0.6622	0.0272
$6s_{1/2}$	0.0413	0.0045	0.1873	0.0098	0.2680	−0.0072	0.3902	0.0102
$6p_{1/2}$	0.0085	0.0006	0.0855	0.0025	0.1100	0.0032	0.1599	0.0057
$6p_{3/2}$	−0.0165	0.0014	0.1057	0.0074	0.1342	0.0102	0.2095	0.0088
Q(Er)	2.332		1.525		1.340		0.975	
ns 1/2	1.9976	0.0001	1.9919	−0.0005	1.989	−0.0025	1.9868	−0.0013
np 1/2	1.8617	0.0414	1.8013	0.0268	1.7965	−0.0079	1.7775	−0.0506
np 3/2	3.7512	0.0262	3.5487	0.0408	3.4942	0.0065	3.3940	−0.0233
Q(X)	−0.610		−0.342		−0.280		−0.158	
Q_{BASIS} (Er)	2.461		1.562		1.388		1.058	
Q_{BASIS} (X)	−0.650		−0.354		−0.292		−0.186	

[a]Reference 23.
[b]Reference 5.
[c]Transition state orbital for all but β orbitals.
[d]Transition state orbital for β orbitals.
[e]He II radiation.
[f]Uncertain.

the moment-polarized orbital results are given for these f orbitals.

In these tables some molecules are calculated with D_{3h} symmetry and others with just C_{3v} symmetry. The connection between molecular orbital symmetry labels for the two corresponding point groups is as follows:

D_{3h}		D_{3h}^{*}		C_{3v}^{*}		C_{3v}
a_1', a_2', e''	↔	$e1$	↔	$e1$	↔	a_1, a_2, e
e', e''	↔	$e3$	↔	$e3$	↔	e
a_1'', a_2'', e'	↔	$e5$	↔	$e1$	↔	a_1, a_2, e

Here the abbreviations $e1$, $e3$, and $e5$ are used for the representation labels $e_{1/2}$, $e_{3/2}$, $e_{5/2}$, respectively, as tabulated, e.g., by Herzberg.[21]

For certain molecules, such as $LaBr_3$ shown in Table IV, C_{3v} and D_{3h} calculations were both performed preserving the metal–halogen distance. There are shifts in energy of 0.1 or less for the individual TSOE's and no change in the order of levels after the proper descent in symmetry correlations have been made. Thus, conclusions can be safely drawn from D_{3h} TSOE calculations when only the metal–halogen distance is known with some certainty. A corollary to this result is that the photoelectron spectrum cannot be used reliably to distinguish D_{3h} or C_{3v} geometry for the neutral lanthanide trihalides. In the five nonrelativistic cases, the results are also listed using the DVM with SCC and the VBHL exchange-correlation potential. For the cases of $CeCl_3$ and $LuCl_3$ the nonrelativistic TSOE's obtained in this work are compared to those obtained by Snow[12] using MS$X\alpha$.

The orbital occupation numbers for the atomic basis orbitals play a fundamental role in the SCC procedure. These occupation numbers determine the potential energy in which the molecular orbital problem is solved. Thus, we have also tabulated the transition state orbital occupation numbers that correspond to the TSOE's listed in Tables IV through IX. For cases in which a moment-polarized calculation is reported, both the moment-density σ and the charge density ρ are listed. By summing over the orbitals corresponding to a particular atom, we obtain the transition state ionicity for these compounds, which is indicated in these tables by $Q(X)$ for halogens and $Q(\mathrm{Ln})$ for cations. These ionicities vary significantly from one halogen to another and show little change within the lanthanide series. The mean cation transition state ionicities calculated were 2.2 for lanthanide fluorides, 1.6 for the chlorides, 1.3 for the bromides and 1.0 for the iodides, with the lutetium compounds displaying a lower ionicity than the mean for all but the fluorides.

Photoelectron spectra are not available for gaseous lanthanide trifluorides. But appearance potentials for certain of these gaseous fluorides have been obtained by electron impact ionization mass spectrometry.[22] The more precise measurements range between 13.0–13.2 eV. X-ray photoelectron spectra have been reported for all the rare earth trifluorides in the solid

TABLE IX. Lutetium trihalides-vertical ionization energies and transition state orbital energies (TSOE).

Halogen		F				Cl					Br					I				
Assignment	PES[a] eV	RDVM -TSOE eV	D_{3h} MO	DVM -TSOE eV	D_{3h} MO	PES[b] eV	RDVM -TSOE eV	C_{3v} MO	DVM -TSOE eV	C_{3v} MO	MSX_α[c] -TSOE eV	PES eV	RDVM -TSOE eV	C_{3v} MO	DVM -TSOE eV	C_{3v} MO	PES eV	RDVM -TSOE eV	D_{3h} MO	DVM -TSOE eV	D_{3h} MO
Xnp_x		13.69	$8e1$	13.85	$2a_2'$	11.55	11.56	$16e1$	11.66	$2a_2$	12.0	10.71	10.65	$16e1$	10.89	$2a_2$	9.57	9.56	$8e1$	9.95	$2a_2'$
		13.77	$7e3$				11.87	$7e3$					10.99	$15e1$			9.87(s)[f]	9.85	$8e5$	10.26	$3a_2'$
		13.78	$8e5$	13.86	$5e'$		11.89	$15e1$	11.86	$7e$	12.1		11.03	$7e3$	11.18	$7e$		9.90	$7e3$		
Xnp_z		13.90	$7e5$	13.92	$3a_2''$	12.05	12.13	$14e1$	12.06	$7a_1$	12.2	11.29	11.18	$14e1$	11.29	$7a_1$	10.14	10.15	$7e5$	10.41	$5e'$
		14.15	$6e3$				12.33	$6e3$					11.40	$13e1$			10.25(?)[g]	10.30	$7e1$		
		14.16	$7e1$	14.29	$2e''$		12.34	$13e1$	12.37	$6e$	12.3	11.50	11.45	$6e3$	11.56	$6e$	10.45	10.49	$6e3$	10.47	$2e''$
																	10.96				
Xnp_σ		14.79	$5e3$	14.90	$4e'$	12.64	12.85	$5e3$	12.78	$5e$	12.4	11.75	11.92	$5e3$	12.08	$5e$	11.03	11.01	$5e3$	11.13	$4e'$
		14.81	$6e5$				12.90	$12e1$				12.09	12.07	$12e1$			11.26	11.28	$6e5$		
		14.91	$6e1$	14.80	$4a_1'$	13.41	13.38	$11e1$	12.86	$6a_1$	12.3	12.79	12.66	$11e1$	12.33	$6a_1$	11.98	11.93	$6e1$	11.51	$4a_1'$
Lu $4f_{7/2}$		18.42	$5e1$	24.14	$3a_1'$		17.26	$10e1$	22.95	$5a_1$	24.3		16.35	$10e1$	22.58	$5a_1$		15.81	$5e5$	22.23	$1e''$
		18.45	$4e1$	24.16	$1a_2'$	17.39[d]	17.39	$9e1$					16.61	$9e1$				15.97	$4e3$		
		18.45	$4e3$	24.21[e]	$3e'$		17.39	$4e3$	22.97[e]	$4e$	24.3	16.8[d]	16.64	$4e3$	22.65	$4e$	16.15[d]	16.23	$5e1$	22.24[e]	$2a_2''$
		18.57	$5e5$				17.46	$8e1$					16.79[e]	$8e1$	22.71[e]	$1a_2$		16.46	$4e1$		
	19																				
Lu $4f_{5/2}$		19.98[e]	$3e1$	24.22	$1e''$		18.96[e]	$7e1$	22.99	$3e$	24.3		18.03	$7e1$	22.71	$3e$		17.53[e]	$4e5$	22.25	$3e'$
		20.02	$3e3$			18.68[d]	18.96	$3e3$	23.01	$1a_2$	24.3	18.4[d]	18.19	$3e3$			17.65[d]	17.70	$3e3$	22.27	$1a_2'$
		20.10	$4e5$	24.30	$2a_2''$		19.00	$6e1$	23.01	$4a_1$	24.4		18.36	$6e1$	22.73	$4a_1$	18.10[d,g](?)	17.83	$3e1$	22.28	$3a_1'$
Xns		31.94	$2e3$	31.89	$2e'$		24.17	$2e3$	23.96	$2e$	23.8		23.45	$2e3$	22.91	$2e$		20.54	$2e3$	19.40	$2e'$
		32.26	$3e5$				24.25	$5e1$					23.50	$5e1$				20.58	$3e5$		
		32.70	$2e1$	32.64	$2a_1'$		24.45	$4e1$	24.18	$3a_1$	23.8		23.66	$4e1$	23.26	$3a_1$		20.77	$2e1$	19.60	$2a_1'$
Lu $5p$		37.96	$2e5$	37.36	$1a_2''$		36.88	$3e1$	36.25	$2a_1$	38.3		36.15	$3e1$	35.88	$2a_1$		35.55	$2e5$	35.30	$1a_2''$
	38	38.27	$1e3$				37.02	$1e3$					36.34	$1e3$				35.72	$1e3$		
		44.96	$1e5$	37.90	$1e'$		43.97	$2e1$	36.46	$1e$	38.4		43.34	$2e1$	36.05	$1e$		42.72	$1e5$	35.57	$1e'$
Lu $5s$		69.39	$1e1$	58.23	$1a_1'$		68.46	$1e1$	57.16	$1a_1$	59.7		67.68	$1e1$	56.77	$1a_1$		67.20	$1e1$	56.30	$1a_1'$

Lutetium trihalides-SCC orbital occupations and basis set ionicities

	Relativistic									Nonrelativistic								
	F		Cl		Br		I			F		Cl		Br		I		
Orbital	ρ	σ	ρ	σ	ρ	σ	ρ	σ	Orbital	ρ	σ	ρ	σ	ρ	σ	ρ	σ
$4f_{7/2}$	5.5032	−0.4958	5.5005	−0.4989	5.9934	−0.0064	5.5009	−0.4995									
									$4f$	13.5004	0.4994	13.5123	−0.4885	13.5054	0.4962	13.4996	0.5001
$4f_{5/2}$	7.9980	−0.0003	7.9988	−0.0006	7.5073	−0.4920	7.9989	−0.1331									
$5s_{1/2}$	1.9990	0.0001	2.0004	0.0001	2.0024	0.0001	2.0030	0.0001	$5s$	1.9985	−0.0000	1.9997	0.0001	1.9997	−0.0001	2.0020	−0.0001
$5p_{1/2}$	2.0006	0.0001	1.9996	0.0001	2.0001	0.0001	1.9990	0.0003									
									$5p$	6.0001	−0.0001	6.0025	0.0001	6.0033	−0.0001	6.0027	−0.0003
$5p_{3/2}$	4.0000	0.0001	3.9984	0.0001	3.9993	0.0002	3.9977	0.0008									
$5d_{3/2}$	0.4665	−0.0025	0.6308	−0.0034	0.6911	−0.0054	−0.7499	−0.0100									
									$5d$	1.1831	0.0040	1.6255	−0.0091	1.7474	0.0096	1.8710	0.0112
$5d_{5/2}$	0.6333	−0.0030	0.8520	−0.0041	0.8946	−0.0062	0.9219	−0.0108									
$6s_{1/2}$	0.1008	−0.0004	0.2946	−0.0008	0.4032	−0.0014	0.5289	−0.0027	$6s$	0.02665	0.0002	0.1568	−0.00051	0.2251	0.0006	0.2998	0.0006
$6p_{1/2}$	0.0414	−0.0002	0.1063	−0.0003	0.1442	−0.0005	0.2210	−0.0013									

TABLE IX (*Continued*)

Orbital	Relativistic F ρ	Relativistic F σ	Relativistic Cl ρ	Relativistic Cl σ	Relativistic Br ρ	Relativistic Br σ	Relativistic I ρ	Relativistic I σ	Orbital	Nonrelativistic F ρ	Nonrelativistic F σ	Nonrelativistic Cl ρ	Nonrelativistic Cl σ	Nonrelativistic Br ρ	Nonrelativistic Br σ	Nonrelativistic I ρ	Nonrelativistic I σ
$6p_{3/2}$	0.0363	−0.0004	0.1328	−0.0005	0.1888	−0.0009	0.3129	0.0021	$6p$	0.0349	0.0004	0.1664	−0.0008	0.2532	0.0008	0.4180	0.0012
Q(Lu)	2.221		1.486		1.176		0.766		Q(Lu)	2.256		1.5369		1.266		0.907	
$ns_{1/2}$	1.9870	−0.0002	1.9925	−0.0001	1.9931	−0.0002	1.9768	−0.0001	ns	1.9903	0.0001	1.9886	−0.0038	1.9883	0.0012	1.9767	0.0000
$np_{1/2}$	1.8677	0.0007	1.8098	0.0009	1.7978	0.0008	1.7801	0.0019									
									np	5.5951	−0.0014	5.3571	0.0033	5.2670	−0.0036	5.1589	−0.0042
$np_{3/2}$	3.7189	0.0003	3.5265	0.0021	3.4343	0.0035	3.3317	0.0068									
Q(X)	−0.5736		−0.3288		−0.225		−0.089		Q(X)	−0.585		−0.346		−0.255		−0.136	
Q_{BASIS} (Lu)	2.134		1.537		1.146		0.749		Q_{BASIS} (Lu)	2.225		1.546		1.270		0.890	
Q_{BASIS} (X)	−0.544		−0.346		−0.216		−0.083		Q_{BASIS} (X)	−0.575		−0.349		−0.257		−0.130	

[a]Reference 23.
[b]Reference 5.
[c]Reference 12.
[d]He II radiation.
[e]Transition state orbital.
[f]Shoulder.
[g]Uncertain.

phase.[23] The problem of establishing an absolute energy scale for the solid state spectra can be overcome by using the gaseous data for calibration of the primarily $F2p^{-1}$ feature at about 13.1 eV and assuming that on the coarser scale of these x-ray photoelectron spectra this $F2p^{-1}$ feature and the $F2s^{-1}$ feature are effectively constant in energy and separated by 21 eV throughout the lanthanide series. This type of calibration is similar to that proposed by Wertheim,[23] but uses gas phase data and results in a 1 eV shift of his energy scale. We take the $F2s^{-1}$ feature to be at 34 eV rather than 33 eV. For LuF_3 we are led to reassign the second most prominent peak observed for this solid as $Lu5p^{-1}$ rather than $F2p^{-1}$, resulting in an additional 4 eV shift in the energy scale for this compound. Thus, the most prominent feature here $Lu4f^{-1}$ occurs at 19 eV rather than 15 eV, which agrees quite well with the DVM-SCC calculations. We have ignored here the finer differences between solid and isolated molecular structure, but this is not unreasonable in light of the broad brush nature of the solid state spectra.

In general, agreement between observed and relativistic DVM-SCC calculated features is quite satisfying, lending confidence to our assignments. The overall width of the valence band ranges from 0.98/0.91 (obs./calc.) for $LaCl_3$ to 2.41/2.37 for LuI_3. This width becomes greater with increasing atomic charge on the lanthanide and halogen atoms, in agreement with the observed PES. Figure 14 shows the comparison between observed and calculated valence bands for $LuCl_3$, $LuBr_3$, and LuI_3. Both relativistic and nonrelativistic DVM-SCC results are shown. The nonrelativistic band width is only some 2/3 of the relativistic calculational or experimental width, which are virtually the same. This type of relativistic width effect is found throughout the lanthanide trihalides.

Focusing on the two extreme molecular orbitals in the valence band, we can see reasons for this change in width. The symmetry requirements for these molecular orbitals are less restrictive in the relativistic case. In particular, these extreme orbitals have the same symmetry type relativistically, although they are of distinct symmetry types nonrelativistically for both D_{3h} and C_{3v} symmetry. The physical effect in the lighter halogens, e.g., chlorine, that causes the relativistic interaction of these molecular orbitals seems to involve primarily 6*s*, 6*p*, and 5*d* orbital bonding with the lanthanide atom. The relativistic 6*s* orbitals of the lanthanides seem to bond far better than the corresponding nonrelativistic 6*s* orbitals: 6*s* participation in the most bound valence orbital is roughly twice as great relativistically as nonrelativistically. It is not possible to ignore however the overlap of the rather diffuse, primarily halogen orbitals with the core orbitals of the lanthanide and the other halogen atoms and the corresponding relativistic influences. The amount of $4f$ electron in the valence orbitals ranges from less than 0.1% for La, Ce, Lu to some 20% for some states of Nd and Er.

In general overall assignment, the nine valence-state ionization potentials fall into two groups of six less

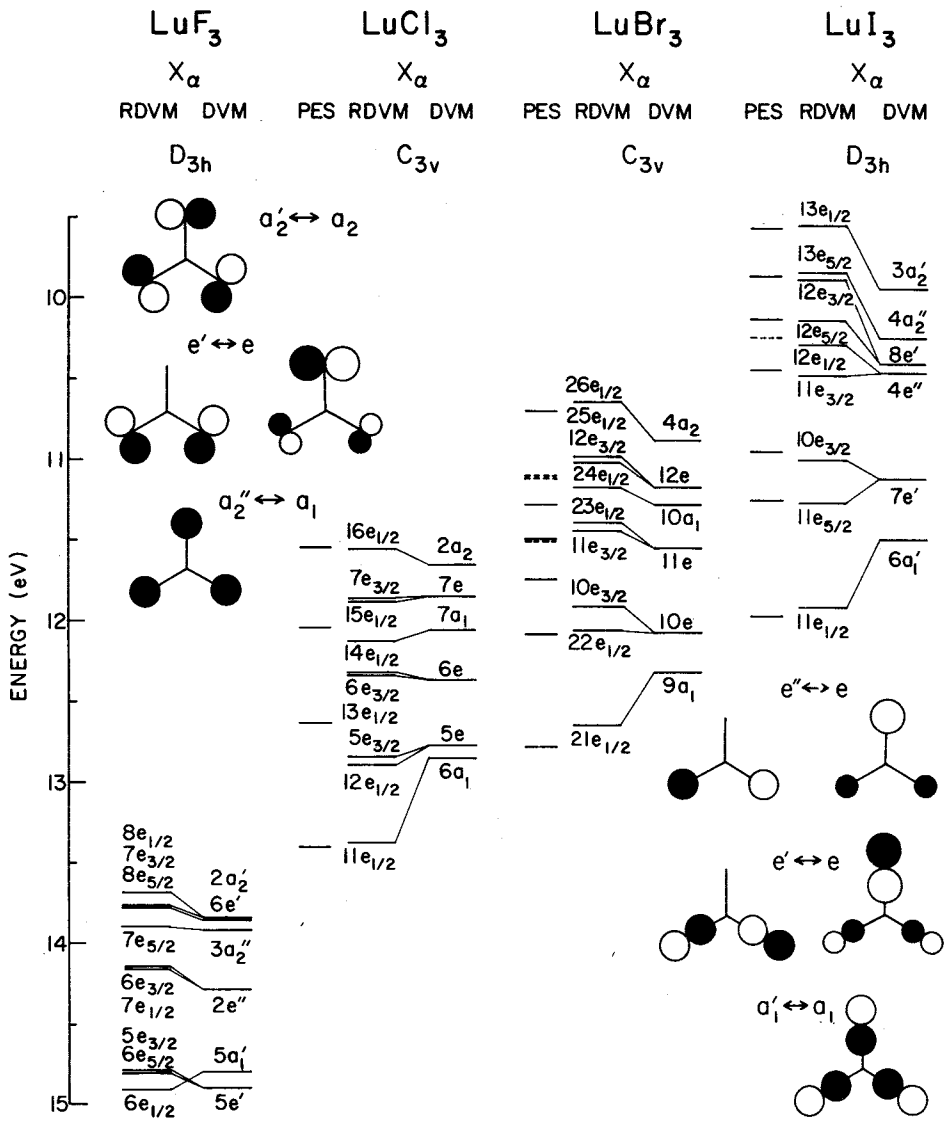

FIG. 14. Orbital diagram for lutetium halides, based on experimental vertical ionization energies (denoted as PES) and on calculated relativistic (RDVM) and nonrelativistic (DVM) transition state orbital energies. The experimental vertical ionization energies for $LuCl_3$ are taken from Ref. 5. Experimental features considered less certain are indicated by dotted lines. The approximate shape of the halogen p valence orbitals is obtained from the calculated nonrelativistic MO coefficients.

bound and three more tightly bound molecular orbitals. For the lighter trihalides (fluorides, chlorides, and bromides) the deeper ionizations correspond to p electrons that are σ-like and the shallower ionizations to the p electrons that are π-like with respect to the halogen–lanthanide bond. For the iodides, spin-orbit splitting is great enough so that these are better described as three $p_{1/2}$ and six $p_{3/2}$ electrons. To illustrate these assignments in detail, Mulliken molecular orbital gross atomic compositions are given in Tables X and XI for $CeCl_3$ and LuI_3, respectively. The two groups of bands A and B, with a rough intensity distribution of 2 to 1 as identified by Lee *et al.*[5] for trichlorides seem well identified as p_π and p_σ electrons.

The general pattern of the valence state photoelectron band shows two trends as a function of the lanthanide for a particular halogen. The first trend shows that the most bound valence orbital steadily splits away from the rest of the valence band on passing from lanthanum to lutetium. This change is reflected in a steady increase in 6s electron involvement in this molecular orbital from 5.3% for LaI_3 to 20.5% for LuI_3 (cf. with 1.4% for $LaCl_3$ to 12.6% for $LuCl_3$) and a steady increase in the overlap bond order between the rare earth and halogen from 7.7% for LaI_3 to 16.5% for LuI_3 (cf. with 3.0% for $LaCl_3$ to 10.1% for $LuCl_3$).

The second trend involves the splitting off of the least bound electron from the rest of the p_π or $p_{3/2}$ group. Here the net effect is the combination of several smaller effects: covalency, spin-orbit splitting, and moment polarization. Thus, the trend is harder to see until one passes beyond gadolinium. In the second half of the lanthanide series the least bound valence molecular orbital remains roughly constant with respect to its lanthanide–halogen overlap bond order while the rest of the p_π or $p_{3/2}$ states are increasing this overlap bond order with higher atomic number and becoming relatively more stable. The net effect is to spread out the p_π subband and split off the first ionization potential. This gives rise to the general patterns of splitting identified in Sec. III above and illustrated in Fig. 10 of Lee *et al.*[5]

TABLE X. $CeCl_3$-C_{3v}-Relativistic polarized calculation.

RDVM -TSOE	Approximate parentage			Bond-orders, %			Atomic orbital Mulliken populations, % Ce							Cl		
eV	Sym	α	β		Ce	Ce-Cl	Cl	5s	5p	5d	$4f_{5/2}$	$4f_{7/2}$	6s	6p	3s	$3p_{1/2}$	$3p_{3/2}$
7.22	$e3$	6e		Ce $4f_{5/2}$	99.7	−0.3	0.6	•••	0.0	1.9	92.0	5.6	•••	0.0	0.0	0.0	0.4
11.36	$e1$	5e			2.5	−0.4	97.9	0.0	0.4	0.1	0.5	0.9	0.0	0.4	0.2	2.6	95.0
11.42	$e3$	5e			4.2	−3.3	99.1	•••	1.1	0.1	0.3	0.4	•••	0.7	0.3	66.3	30.8
11.43[a]	$e1$	$1a_2$		Cl	2.8	−0.9	98.1	0.0	0.5	0.1	0.7	0.5	0.0	0.6	0.2	37.0	60.4
11.49	$e1$		5e	$3p_\pi$	2.5	−1.0	98.5	0.0	0.5	0.1	0.3	0.6	0.0	0.4	0.2	1.8	96.1
11.54	$e3$		5e		4.4	−4.0	99.6	•••	1.3	0.1	0.2	0.3	•••	0.5	0.3	67.0	30.3
11.55	$e1$		$1a_2$		2.5	−1.1	98.6	0.0	0.5	0.1	0.5	0.4	0.0	0.4	0.2	37.0	60.8
11.62	$e1$	$5a_1$			3.3	1.9	94.8	0.0	0.4	2.2	0.3	0.2	0.3	0.9	0.1	33.9	61.8
11.74	$e1$		$5a_1$		3.2	1.2	95.6	0.0	0.4	2.0	0.2	0.1	0.2	0.8	0.1	33.7	62.5
11.80	$e3$	4e		Cl	5.3	7.5	87.2	•••	0.2	8.6	0.2	0.1	•••	−0.1	0.0	20.8	70.1
11.81	$e1$	4e		$3p_z$	5.1	7.9	87.0	0.0	0.1	8.6	0.1	0.2	0.0	0.0	0.1	20.0	70.9
11.91	$e3$		4e		4.8	6.9	88.3	•••	0.2	7.8	0.1	0.1	•••	−0.1	0.0	21.0	70.7
11.92	$e1$		4e		4.6	7.3	88.2	0.0	0.1	7.8	0.1	0.2	0.0	0.0	0.1	20.3	71.4
12.15	$e3$	3e			12.4	8.7	78.9	•••	1.1	14.8	0.6	0.2	•••	0.1	1.9	6.5	74.8
12.20	$e1$	3e			10.7	5.0	84.3	0.2	0.6	9.8	0.5	0.7	1.2	0.1	2.3	27.7	56.8
12.24	$e3$		3e	Cl	11.6	8.3	80.0	•••	1.2	13.8	0.4	0.2	•••	0.1	1.7	5.9	76.6
12.27	$e1$	$4a_1$		$3p_\sigma$	9.8	4.2	86.0	0.2	0.4	8.5	0.4	0.9	1.5	0.0	2.5	60.9	24.7
12.29	$e1$		3e		10.1	4.6	85.2	0.2	0.7	9.4	0.4	0.6	1.1	0.1	2.1	29.0	56.5
12.36	$e1$		$4a_1$		9.2	3.5	87.3	0.2	0.4	7.9	0.3	0.7	1.4	0.0	2.4	61.7	25.0

[a]Transition state orbital.

TABLE XI. LuI_3-D_{3h}-relativistic polarized calculation.

RDVM -TSOE	Approx. parentage		Bond orders, %			Atomic orbital Mulliken populations, % Lu							I		
eV	Sym	α	β	Lu	Lu-I	I	5s	5p	5d	$4f_{5/2}$	$4f_{7/2}$	6s	6p	$5s_{1/2}$	$5p_{1/2}$	$5p_{3/2}$
9.56	$e1$		$Ip_{3/2}$	2.9	2.5	94.6	0.0	•••	3.8	0.0	0.0	0.3	•••	0.0	7.6	88.2
9.60	$e1$	$Ip_{3/2}$		2.8	2.5	94.7	0.0	•••	3.7	0.0	0.0	0.3	•••	0.0	7.4	88.5
9.85	$e5$		$Ip_{3/2}$	4.7	11.5	83.8	•••	0.0	3.6	0.0	0.0	•••	6.8	0.0	2.7	86.8
9.85	$e5$	$Ip_{3/2}$		4.7	11.4	84.0	•••	0.0	3.6	0.0	0.0	•••	6.7	0.0	2.6	87.0
9.90	$e3$		$Ip_{3/2}$	7.9	11.8	80.3	•••	0.0	11.0	0.0	0.0	•••	2.7	0.1	0.0	86.1
9.90	$e3$	$Ip_{3/2}$		7.7	11.6	80.7	•••	0.0	10.7	0.0	0.0	•••	2.7	0.1	0.0	86.4
10.15	$e5$		$Ip_{3/2}$	4.7	10.8	84.6	•••	0.0	0.0	0.0	0.0	•••	9.9	1.1	10.8	78.1
10.15	$e5$	$Ip_{3/2}$		4.6	10.7	84.7	•••	0.1	0.0	0.0	0.0	•••	9.9	1.1	10.7	78.2
10.30	$e1$	$Ip_{3/2}$		7.9	9.3	82.8	0.0	•••	10.4	0.0	0.0	2.2	•••	0.3	38.0	49.1
10.31	$e1$		$Ip_{3/2}$	8.1	9.4	82.5	0.0	•••	10.6	0.0	0.0	2.2	•••	0.3	38.0	49.1
10.49	$e3$	$Ip_{3/2}$		14.7	15.6	69.8	•••	0.0	21.6	0.0	0.0	•••	0.9	0.6	19.1	57.9
10.50	$e3$		$Ip_{3/2}$	14.9	15.6	69.5	•••	0.0	21.8	0.0	0.0	•••	0.9	0.6	19.8	56.9
11.01	$e3$	$Ip_{1/2}$		8.0	6.5	85.6	•••	0.2	7.6	0.0	0.1	•••	3.3	2.2	72.5	14.1
11.01	$e3$		$Ip_{1/2}$	8.2	6.6	85.2	•••	0.2	7.9	0.0	0.1	•••	3.3	2.3	71.7	14.6
11.28	$e5$	$Ip_{1/2}$		11.0	12.0	77.1	•••	0.0	16.3	0.0	0.0	•••	0.6	2.2	72.2	8.6
11.29	$e5$		$Ip_{1/2}$	11.2	12.1	76.7	•••	0.0	16.6	0.0	0.0	•••	0.6	2.2	71.9	8.7
11.94	$e1$	$Ip_{1/2}$		15.8	16.5	67.7	0.1	•••	3.3	0.0	0.2	20.5	•••	5.4	42.6	27.8
11.94	$e1$		$Ip_{1/2}$	16.0	16.5	67.5	0.1	•••	3.3	0.0	0.2	20.7	•••	5.5	42.4	27.9
15.76[a]	$e5$	$f_{7/2}$		99.9	0.0	0.1	•••	−0.2	0.0	0.2	99.9	•••	0.0	0.0	0.0	0.0
15.92	$e3$			99.8	0.0	0.2	•••	0.0	0.0	0.8	99.1	•••	0.0	0.1	0.1	0.0
16.15	$e5$		$f_{7/2}$	99.9	0.0	0.1	•••	−0.2	0.0	0.1	100.0	•••	0.0	0.0	0.0	0.0
16.18	$e1$	$f_{7/2}$		99.7	0.0	0.3	0.0	•••	0.0	0.3	99.4	0.0	•••	0.1	0.1	0.0
16.31	$e3$		$f_{7/2}$	99.9	0.0	0.2	•••	0.0	0.0	0.9	99.0	•••	0.0	0.1	0.1	0.1
16.40	$e1$	$f_{7/2}$		99.8	0.0	0.1	0.0	•••	0.0	0.0	99.9	0.0	•••	0.1	0.0	0.0
16.57	$e1$		$f_{7/2}$	99.7	0.0	0.3	0.0	•••	0.0	0.3	99.5	0.0	•••	0.2	0.1	0.0
16.80	$e1$			99.9	0.0	0.1	0.0	•••	0.0	0.0	99.9	0.0	•••	0.1	0.0	0.0
17.48	$e5$			99.9	0.0	0.1	•••	−0.1	0.0	99.8	0.2	•••	0.0	0.1	0.0	0.0
17.64	$e3$	$f_{5/2}$		99.9	0.0	0.1	•••	0.0	0.0	99.2	0.8	•••	0.0	0.0	0.0	0.0
17.78	$e1$			99.7	0.0	0.4	0.0	•••	0.0	99.4	0.3	0.0	•••	0.3	0.0	0.1
17.87	$e5$			99.9	0.0	0.2	•••	−0.1	0.0	99.8	0.1	•••	0.0	0.1	0.0	0.0
18.05	$e3$		$f_{5/2}$	99.9	0.0	0.1	•••	0.0	0.0	99.1	0.9	•••	0.0	0.1	0.0	0.0
18.18	$e1$			99.6	0.0	0.4	0.0	•••	0.0	99.4	0.2	0.0	•••	0.4	0.0	0.0

[a]Transition state orbital.

The intensity patterns and their changes between the He I and He II spectra are semiquantitatively explained by the relativistic DVM-SCC calculations. The He I intensities seem to be roughly equal for all of the valence band states, which consist rather uniformly of ~75% or more halogen np wave functions, where $n = 3, 4, 5$ for chlorine, bromine, and iodine, respectively. The distribution of calculated TSOE's leads to a piling up of intensity in the low energy part of the band where the six p_π states fall. The other three p_σ states give the second major feature of the spectra. For early members of the series (lanthanum through gadolinium) where the individual components of the p_π subband are not resolved this gives the characteristic roughly two to one intensity pattern.

For He II spectra the fractions of $6s$, $5d$, and $4f$ rare earth orbital participation seem to be controlling the relative intensities within the valence band, as was speculated by Lee *et al.*[5] The orbital analyses given in Tables X and XI for $CeCl_3$ and LuI_3, respectively, are typical of the results for our DVM-SCC calculations. These show variations among the molecular orbitals for $6s$ and $4f$ participation in $CeCl_3$ of 0.0% to 1.5% and 0.23% to 1.4%, respectively; and, in LuI_3 of 0.0% to 20.7% and 0.0% to 0.2%. The corresponding variation of $5d$ orbital participation is 0.1% to 14.2% in $CeCl_3$ and 0.0% to 21.7% in LuI_3. This amount of $5d$ orbital participation is substantially greater than that reported by Snow[12] for the MS$X\alpha$ results. The distribution of the $5d$ orbital involvement gives the smallest $5d$ character to the least bound p_π orbitals and most $5d$ character to the strongly bound p_σ orbitals. The rough equality of total $5d$ character in the p_π and p_σ subbands leads to more nearly equal intensities for these subbands in the He II spectra. Difficulties of resolving the experimental peaks together with uncertainties about the relative ionization cross sections for np, $4f$, $6s$, and $5d$ wave functions in these molecules make it seem unreasonable to give still more detailed assignments of intensities at this time.

Comparison of results of D_{3h} and C_{3v} calculations for $CeBr_3$ make it seem highly unlikely that d-orbital intensity distribution calculations can shed light on the question of planarity for the lanthanide trihalides as Lee *et al.*[5] had suggested. In the relativistic DVM-SCC calculation, the fraction of d orbital participation in the most bound valence orbital is not particularly sensitive to the planarity—5.8% vs 8.4% for planar and nonplanar, respectively.

It seems noteworthy that the rather substantial amount of $6s$ participation in this most bound valence orbital is probably of importance in understanding the enhancement of this feature in the He II spectrum. For $LuCl_3$ the percent atomic orbital character for the deepest three molecular orbitals is $5e3$: 0.0, 16.9, 0.2; $12e1$: 0.1, 14.7, 0.2; and $11e1$: 12.6, 2.4, 0.5, for $6s$, $5d$ and $4f$, respectively. In energy the first two molecular orbitals together correspond to peak B and the last to peak B' in Fig. 7 of Lee *et al.*[5] The marked enhancement of the peak B' in their He II spectrum can only be explained in terms of these atomic compositions if the $6s$ wave function has an appreciably enhanced He II relative cross section. Lee *et al.*[5] have commented on this possibility of $6s$ involvement based on the work of Egdell and Orchard for $HfCl_4$.[24]

Concerning the assignment of the p_σ molecular orbitals in the nonrelativistic calculation for planar symmetry, Lee *et al.*[5] decided by analogy with InI_3 that these orbitals should be labeled as symmetries a_1' and e'. We agree with this assignment as illustrated by the D_{3h} nonrelativistic results for LuF_3 and LuI_3 in Table IX and in Fig. 14.

In passing we have also carried out DVM-SCC calculations using the VBHL exchange-correlation potential for InI_3 both relativistically and nonrelativistically. The level of agreement of TSOE's with experimental energies is quite good, within ±0.12 eV at most. In summary, we have confirmed the general, qualitative features of previous assignments[25] for InI_3. From the Mulliken population analysis we can predict that only the photoelectron peak near 14 eV should have enhanced intensity for He II radiation, since it has about 50% In5s character. The $4d$ involvement is quite small (less than 0.4%) for photoelectron energies less bound than 15 eV.

Turning now to the primarily $4f$ orbitals, we note that even moment-polarized calculations do not give the details corresponding to final state multiplet structures. Only for the cerium and lutetium trihalides is the final state well described by a single determinant wave function so that the TSOE's give good indications of the photoelectron peaks. For the other, open shell f electron systems only some "average" energy of the fine structure components is indicated by the present TSOE's. Only for very low resolution, high photon energy spectra such as those for the lanthanide fluorides[23] do these average energies give an indication of the observed photoelectron peaks. Our studies do make clear that the $4f$-orbital ionization energies are quite close to those of the halogen valence orbitals for most of the lanthanide trihalides. The $4f$ orbitals however occupy a distinct spatial region of these molecules, giving rise to only limited interaction with the halogen orbitals. As a measure of the spatial extent of the lanthanide orbitals we can look at the value of r at which the function $r\psi$ reaches its maximum. For the major component of the $4f_{7/2}$ orbital this maximum occurs at ~0.4 Å for $La^{+1.5}$ and ~0.3 Å for $Lu^{+1.01}$. These values can be compared to those for $5d_{5/2}$, $6p_{3/2}$ and $6s_{1/2}$ orbitals: 1.22, 2.27, and 1.89 Å for $La^{+1.5}$. Moreover, the charge density of this $4f$ orbital for lanthanum is quite tightly constrained to a narrow shell between ~0.2 and ~0.7 Å. This situation gives the $4f$ orbital a rather low binding energy but also a low chemical activity.

It is important to note that the preceding observations are based on transition state orbital features. Ground state molecular properties should properly be compared with ground state orbital features. Some exploratory calculations do show however that the ground state orbital compositions are in general close to the transition state orbital compositions, provided allowance is made for the reordering of orbital ener-

gies. In a few special cases, there arises an accidental degeneracy of a primarily $4f$ orbital with a halogen orbital, resulting in a large, arbitrary mixing of these molecular orbitals. In general, however, we can reasonably draw at least preliminary inferences about ground state orbital properties based on transition state orbital calculations for the lanthanide trihalides.

In summary, the picture of the electronic structure for the lanthanide trihalides that emerges from our studies is that of highly ionic molecules, evidenced by the small overlap bond orders between halogen and lanthanide atoms. The $4f$ electrons and the halogen valence electrons occupy quite separate physical regions of the molecule. What covalency there is arises primarily from the rare earth $5d$, $6s$, and $6p$ involvement, which reduces the effective ionicity to between ~ +1.0 and ~ +2.2 depending on the particular compound. The optimized minimal atomic basis set together with the self consistent charge approximation gives remarkably consistent (perhaps to some extent fortuitous) agreement with the observed photoelectron features.

V. COMPARISON OF ELECTRON IMPACT MASS SPECTRA AND PHOTOELECTRON SPECTRA OF THE LANTHANIDE TRIHALIDES

Mass spectrometric studies have been performed on all of the lanthanide trifluorides except PmF_3.[22] The parent ion LnF_3^+ is vanishingly small (barely detectable) in all cases. The enthalpy of atomization $[LnF_3(g) \rightarrow Ln(g) + 3F(g)]$ displays a variation along the lanthanide series (see Fig. 15) which is similar to that observed in the diatomic LnO species[26] and has been correlated with the $4f^n \rightarrow 4f^{n-1}\,5d$ excitation necessary to produce the proper valence state (or hybridization) in those lanthanide atoms having $4f^n 6s^2$ ground state configurations. (The thermochemical data for the lanthanide fluorides are not as precise as they appear to be for the corresponding chlorides and iodides, where the pattern across the lanthanide series more closely resembles that with the oxides.)

The average enthalpy of atomization for the lanthanide fluorides is about 420 kcal/mol. The available evidence[22] indicates that the successive removal of F atoms from LnF_3 requires approximately equal amounts of energy. We can therefore roughly estimate the bond energy for the first dissociation $[LnF_3(g) \rightarrow LnF_2(g) + F(g)]$ as ~ 140 kcal/mol or ~ 6.07 eV.

For the lanthanide chlorides, some parent $LnCl_3^+$ ion is observed, although the first fragment $LnCl_2^+$ is substantially more intense at 50 eV electron energy.[27] The difference in A. P. between MCl_3^+ and MCl_2^+ has been reported to be -0.2 ± 1 eV ($LaCl_3$), $+1.0 \pm 0.6$ eV ($LuCl_3$), and $> +0.5 \pm 0.3$ eV ($NdCl_3$). The enthalpies of dissociation into free atoms $[LnCl_3(g) \rightarrow Ln(g) + 3Cl(g)]$ (see Fig. 15) taken from Ref. 28 clearly display the characteristic variation across the lanthanide series mentioned earlier. The average atomization energy is about 325 kcal; assuming equal bond strengths, the bond energy for the first dissociation $[LnCl_3(g) \rightarrow LnCl_2(g) + Cl(g)]$ is ~ 108 kcal/mol or ~ 4.70 eV.

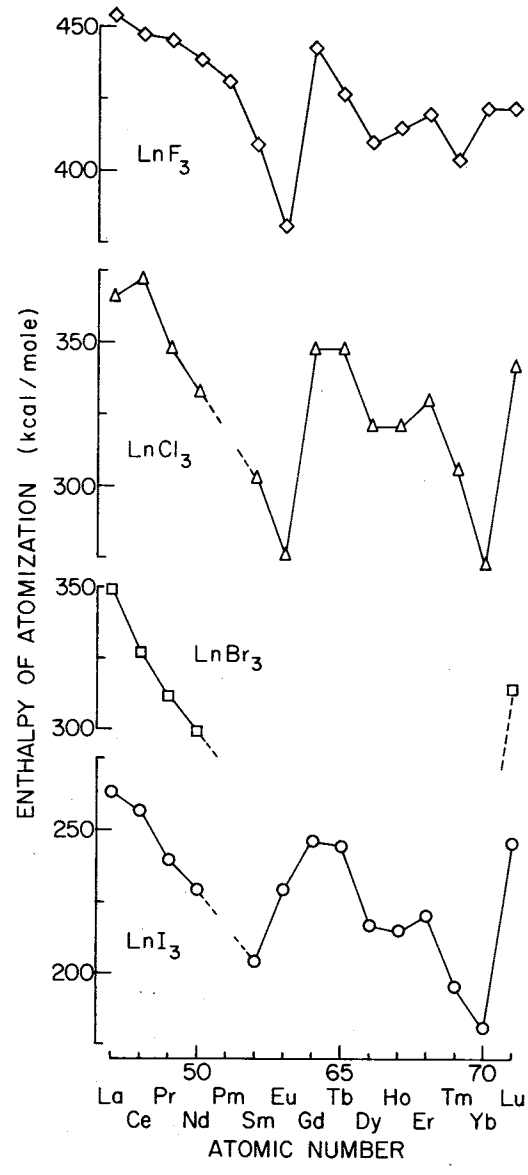

FIG. 15. The enthalpies of dissociation into free atoms for lanthanide halides. The data are taken from Refs. 22, 28, 20, and 30 for the fluorides, chlorides, bromides and iodides, respectively. The enthalpies of atomization display a characteristic variation along the lanthanide series, similar to that observed (Ref. 26) in the diatomic LnO species.

Corresponding information on lanthanide bromides is very sketchy. Enthalpies of dissociation into free atoms are available for the first four members and for $LuBr_3$.[20] The characteristic decline between $LaBr_3$ and $NdBr_3$ can be noted in Fig. 15.

An average atomization energy of about 290 kcal/mol is estimated for $LnBr_3$. Our assumption of equal bond strengths leads to ~ 96.7 kcal/mol (~ 4.19 eV) for the bond energy of the first dissociation. Mass spectrometric studies have been reported[29] for $NdBr_3$ (no parent ion observed), $YbBr_3$ (parent ion barely observed, too weak for A. P. measurement) and $TmBr_3$, where a significant parent ion intensity with an appearance potential 1.5 ± 1 eV lower than that for $TmBr_2^+$, was observed.

Fairly extensive work on the lanthanide tri-iodides exists, largely due to Hirayama and co-workers.[30,31] The enthalpies of dissociation for all triodides except PmI_3 are shown in Fig. 15. The characteristic variation along the lanthanide series noted earlier is well defined in the iodides. The average value of the energy of dissociation into free atoms is ~ 228 kcal/mol, corresponding to ~ 76 kcal/mol (~ 3.30 eV) per bond. Parent ions have been observed for all of the lanthanide iodides studied, although LnI_2^+ is the most abundant in every instance. The abundances have been measured at 28 eV electron energy. The ratio of intensities of $LnI_3^+ : LnI_2^+$ is 0.14 ± 0.03 in the series between LaI_3 and NdI_3, then increases abruptly at GdI_3 and remains ~ 0.5. The difference in appearance potentials between LnI_3^+ and LnI_2^+, according to the data of Hirayama *et al.* oscillates in the first series members (0.8, 0.1, 0.8, 0.1 eV for LaI_3, CeI_3, PrI_3, NdI_3) then displays a gradual increase between GdI_3 and TmI_3 from 0.9 to 1.3 eV. The experimental error given varies between ± 0.2 and ± 0.5 eV.

The discussion to be presented below will attempt to correlate and systematize the above information by making use of our photoelectron spectra. At the outset, we must recognize that at least 1/3 of the ion abundances reported in the mass spectra of the iodides at 28 eV occur as LnI^+ and Ln^+. The appearance potentials given for these ions are at higher energy than the valence bands observed in the photoelectron spectra. Therefore, the origin of LnI^+ and Ln^+ must be electronic states of LnI_3^+ between ~ 13–28 eV which are extremely weak or undetectable in the photoelectron spectra. They are most likely *not* the ionizations due to f-electron emission. The most abundant relative intensities of LnI^+ and Ln^+ occur for LaI_3, where the f electron contribution is nil. In addition, the ejection of f electrons requires the surmounting of a centrifugal barrier. With 28 eV electron impact, the f electron ejection would be largely suppressed, relative to ligand or metal "s"- or "p"-like orbitals. Hence, the energy region between ~ 13–28 eV must be accessed by low energy electrons via electric-dipole forbidden processes rather efficiently. The nature of these states is not clear, but calculations indicate that ligand s-like and lanthanide $5p$-like orbitals would require energies in this range for electron ejection.

We shall make two simplifying assumptions in the ensuing discussion.

(1) The $LnX_3 \rightarrow LnX_2 + X$ potential energy surface, and that for $LnX_3^+ \rightarrow LnX_2^+ + X$ can be described in quasidiatomic fashion.

(2) The primary source of the LnX_3^+ and LnX_2^+ ions are the ionic states observed in the VUV photoelectron spectra.

A schematic, quasidiatomic potential energy diagram is shown in Fig. 16. Some energies relevant to the discussion are also sketched on this diagram. Although our $X\alpha$ calculations yield a net charge on Ln^+ considerably less than three (but more than one in most cases), the major contribution to bonding must be electrostatic, since the overlap integrals, which are criteria for covalent bonding, are very low. The low energy ionizations are from molecular orbitals centered on the halogens (X^- type), and if localized on a particular halogen, will significantly weaken the $Ln^+ - X^-$ bond. For purely ionic bonding, the loss of an electron from X^- will cause a loss in that Ln–X bond strength of order (Ze^2/r) (where Z, the charge on Ln^+, is of order 1.5, and r is the internuclear distance), and retention of an ion-induced dipole bond strength of order $(Z\alpha e^2/2r^4)$, α being the polarizability. (This approach should be most applicable to the lanthanide fluorides, and successively less so for the heavier halides.) If we approximate the potential energy W of the $Ln^+ - X^\circ$ bond with a Lennard-Jones type of repulsive potential (c/r^{12}) and the aforementioned attractive potential, then

$$W = \frac{c}{r^{12}} - \frac{Z\alpha e^2}{2r^4} .$$

Using the equilibrium criterion

$$\frac{\partial W}{\partial r} = 0$$

leads to the expression

$$W = -\frac{Z\alpha e^2}{3r_0^4} ,$$

where r_0 is the equilibrium internuclear distance. Taking $Z \sim 1.5$, $\alpha = 0.57$, 2.3, 3.4, and 5.7 $(\text{Å})^3$ for F, Cl,

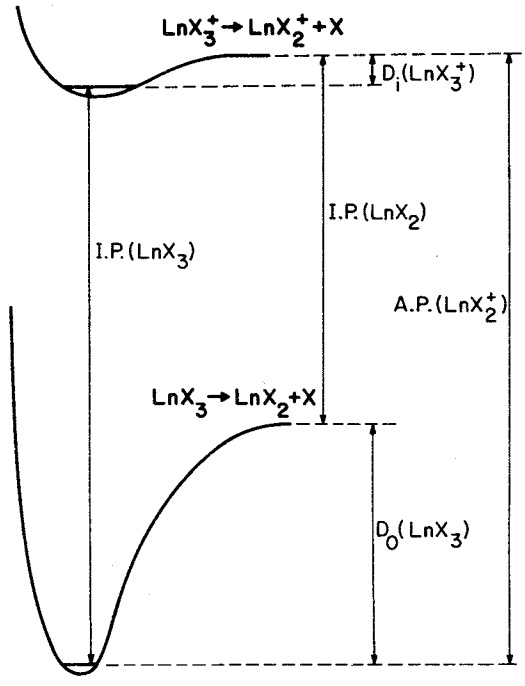

FIG. 16. Quasidiatomic potential energy diagram for the ground states of a lanthanide trihalide neutral molecule LnX_3 and the corresponding molecular ion LnX_3^+. The diagram shows the relationship between the ionization potential of the trihalide, I.P. (LnX_3) and dihalide molecule, I.P. (LnX_2), as well as the appearance potential for the dihalide ion, A.P. (LnX_2^+) and the energy of dissociation for the $LnX_3 \rightarrow LnX_2 + X$ process, $D_0(LnX_3)$ and for the $LnX_3^+ \rightarrow LnX_2^+ + X$ process, $D_i(LnX_3^+)$.

TABLE XII. Dissociation energies D_i (LnI_3^+) for the process $LnI_3^+ \rightarrow LnI_2^+ + I$.

	Hirayama *et al.*[a]	Graphical integration of PES	Ion-induced dipole calculation
LaI_3	0.8 eV	0.595 eV	0.54 eV
CeI_3	0.1	0.645	0.56
PrI_3	0.8		0.57
NdI_3	0.1	0.556	0.58
GdI_3	0.9		0.63
TbI_3	1.0		0.64
DyI_3	1.0		0.65
HoI_3	1.0		0.66
ErI_3	1.2	1.169	0.67
TmI_3	1.3		0.68
LuI_3		1.055	0.70

[a]References 30 and 31.

Br, and I, respectively and average r_0 (Ln–X) values of 2.1, 2.5, 2.65, and 2.85 Å for X = F, Cl, Br and I,[32] we obtain $D_i(LnX_3^+) = 0.21$, 0.42, 0.50, and 0.62 eV for typical Ln^+–F, Ln^+–Cl, Ln^+–Br and Ln^+–I bonds.

Apart from the assumptions already made, this crude approach is subject to other criticisms. The critical internuclear distance has been taken to be that in the neutral molecule, whereas it is expected to be longer in the molecular ion. The Franck–Condon region will accentuate higher vibrational levels in the molecular ion, rather than the ground state level. At 1000 K, the vibrational heat contents of LaF_3, $LaCl_3$, $LaBr_3$, and LaI_3 are 9.5, 10.5, 10.9, and 11.2 Kcal/mol, respectively. Each have a rotational heat content of 2.98 kcal/mol, which is also likely to be available for dissociation. (Not all of the vibrational energy will be available—it depends upon Franck–Condon factors.) From the foregoing discussion, it is not surprising that the LnF_3^+ ions are not observed. If the bond strength is 0.21 eV and the rotational energy at the experimental temperature (~ 1400 K) is 0.18 eV, very few parent ions would survive. For the chlorides, the bond strength is approximately twice as large, and some parent ions are expected. The iodides, as anticipated, apparently have the largest fraction of parent ions.

We have attempted to use the relative intensities of LnI_3^+ : LnI_2^+ from the data of Hirayama *et al.*[30,31] together with our photoelectron spectra, to arrive at a better measure of the Ln^+–I bond strengths than was possible from their appearance potential measurements. The assumption here is that 28 eV electrons will produce approximately the same ratio of valence states as are formed in our 21.2 eV photoelectron spectra. Electron impact ionization cross sections generally increase linearly with excess energy from threshold to a few tens of eV. Since our valence bands span the region ~9–12 eV, the assumption of linear behavior to 28 eV (with approximately equal slopes—a fair estimate since these orbitals are all similar, halogen p-like) would predict comparable intensities of valence bands, perhaps accentuating the lower ionization region. Hence, we have integrated the photoelectron valence spectra, apportioned the areas to match the relative intensities of Hirayama *et al.*[30,31] and at the appropriate area deduced a threshold for LnX_2^+. [For LuI_3 (for which mass spectral data were unavailable), we used the relative intensities of TmI_3.]

The adiabatic thresholds for LnI_3^+ were approximated by the position where 0.4% of the area of the valence band is attained. This is an objective, though imprecise manner for taking into account the hot bands, which give rise to an exponential tail at threshold. The 0.4% criterion approximately corresponds to the onset of a linear increase of intensity in the first photoelectron band. The results are shown in Table XII, together with ion-induced dipole calculations using $Z = 1.5$, $\alpha = 5.7(\text{Å})^3$ and internuclear distances taken from Hargittai.[32] Also shown are the appearance potential measurements of Hirayama *et al.*[30,31]

The graphical integration procedure generates a more gradual progression of dissociation energies. The ion-induced dipole calculation simulates the values from graphical integration for the earlier members, but does not seem to increase as rapidly along the lanthanide series, implying an attractive force with higher r dependence than r^{-4}.

By combining our graphically calculated appearance potentials for LnI_2^+ with experimental atomization energies, and assuming equal bond strengths for the three bonds, we can estimate the ionization potential of the diiodides, I.P. (LnX_2). The results, shown in Table XIII, are relatively low values (~ 5.6–6.9 eV), closely comparable to the atomic ionization potentials[33] (also shown in Table XIII). By contrast, the directly measured I.P.'s for EuI_2 and SmI_2 are about 2 eV higher.[31,34] One probable source of discrepancy in this case is our assumption of equal bond strengths for the three bonds. The LnI_2–I bond is apparently weaker than the other two. Another is that reported electron impact appearance potentials frequently are higher than those determined spectroscopically or by photoionization.

Some further insight about bonding can be elicited from the photoelectron spectra of the lanthanide chlor-

TABLE XIII. Inferred and observed ionization potentials for lanthanide diiodides (eV).

	I.P. (LnI_2)	I.P. (Ln)[d]
$LaI_2 \rightarrow LaI_2^+$	5.58[a]	5.557
$CeI_2 \rightarrow CeI_2^+$	5.76[a]	5.539
$NdI_2 \rightarrow NdI_2^+$	6.05[a]	5.525
$ErI_2 \rightarrow ErI_2^+$	6.91[a]	6.108
$LuI_2 \rightarrow LuI_2^+$	6.63[a]	5.426
$EuI_2 \rightarrow EuI_2^+$	8.85 ± 0.2[b]	
$SmI_2 \rightarrow SmI_2^+$	9.0 ± 0.2[c]	

[a]Inferred, this work, assuming equal bond strengths for successive removal of the three iodine atoms.
[b]Observed, Ref. 34.
[c]Observed, Ref. 31.
[d]Reference 33.

ides. We have extracted adiabatic ionization potentials from the published spectra,[5] which vary more-or-less smoothly from ~10.6 eV for $LaCl_3$ to ~11.2 eV for $LuCl_3$. From Fig. 16, the ionization potential of $LnCl_2$ would be approximated as: I.P. $(LnCl_2)$ = I.P. $(LnCl_3) - D_0(LnCl_3) + D_i(LnCl_3^+)$. For the case of europium chloride, we take I.P. $(EuCl_3) \cong 11.0$ eV, $D_0(EuCl_3) \cong 4.0$ eV (from Fig. 15) and $D_i(EuCl_3^+) \cong 0.4$ eV (previous ionic model estimate). These estimates lead to I.P. $(EuCl_2) \cong 7.4$ eV, whereas the spectrum of $EuCl_2$ reported by Lee *et al.*[5] reveals an adiabatic ionization potential of ~ 9.5 eV. The directly measured ionization potential is about 2 eV higher than that resulting from the simple model assuming equal bond strengths, as we noted in the case of the lanthanide iodides. In this case, the larger error introduced by electron impact appearance potential measurements is absent. The most likely source of discrepancy in this analysis is our assumption of equal bond strengths for the three bonds. The implication is that the third bond is substantially weaker in the lanthanide chlorides and iodides (and by inference, the bromides), whereas it is of comparable strength in the fluorides.

Our tentative interpretation is that the bonding in the fluorides is predominantly ionic. For the other halides, covalent contributions become progressively more important. This requires $4f^n \rightarrow 4f^{n-1}\,5d$ promotion and hybridization, the cost of promotion appearing in the weaker third bond.

VI. CONCLUSIONS

Experimentally, it has been shown that in early members of the lanthanide trihalide molecules, the $4f$-like ionizations have lower ionization energies than the ligand p-like orbitals, whereas in late members of this series, the $4f$-like ionizations are more bound, ultimately becoming corelike. Superficially, this parallels the behavior of the metal $3d$-like orbitals in the dihalides of the first transition metal series. However, the $3d$-like features in the transition metal dihalides are observed in He I spectra, whereas the $4f$-like ionizations in the lanthanide trihalides are vanishingly small in the He I PES becoming observable in He II PES and dominant in x-ray PES. This wavelength dependence of relative cross sections is presumably attributable to the larger centrifugal barrier toward f electron ejection. As a consequence, the ligand valence band is clearly separable from the f-like ionizations in the He I spectra of the lanthanide trihalides, enabling us to focus on the detailed fine structure of this valence band and its variation with halogen and lanthanide. The success of the $X\alpha$ DVM-SCC calculation reported here, particularly for the open-shell systems, is at least partly attributable to the disjoint regions of space occupied by lanthanide $4f$-like and halogen p-like orbitals. This enables one to use transition state orbital energies to calculate the details of the valence band in the average field of the $4f$ electrons, without explicit consideration of the open-shell multiplet fine structure. This essentially one-electron model cannot be expected to provide such accuracy for open-shell systems in general, and particularly not for the transition metal dihalides, where the metal $3d$-like and halogen p-like orbitals are in closer spatial proximity.

A consequence of the good agreement between calculational and experimental ionization energies is that it provides confidence in the wave functions of the $4f$-like orbitals, which are found to be restricted to a thin shell and excluded from the valence region. It is this spatial distribution of $4f$-like orbitals, rather than their binding energy, which explains their chemical inertness.

By contrast, we find that the lanthanide $5d$ and $6s$ orbitals are involved in chemical bonding, as evidenced by the appreciable overlap between these orbitals and the halogen outer p orbitals. In the ground states of the lanthanide atoms, only La, Ce, Gd, and Lu have occupied $5d$ orbitals. In order to achieve the favorable $5d$ bonding properties, it is necessary for the other lanthanide atoms to undergo $4f \rightarrow 5d$ promotion. It is this promotional energy which becomes the characteristic variation in bond energy across the lanthanide series (Fig. 15) as already noted by previous workers.[26]

The relative ionization energies and widths of the valence bands calculated by the $X\alpha$ DVM-SCC transition state method for these heavy element systems are the same quality as for lighter ones, provided that one uses relativistic atomic wave functions and relativistic molecular kinetic energies. However, in order to achieve more accurate absolute energies and reliable ordering of close-lying levels it is necessary to use the von Barth–Hedin–Lundqvist local moment-density potential, which takes into account correlation as well as exchange in the interelectronic potential. The diffuseness of the halogen p valence orbitals makes their energies particularly sensitive to correlation energy and the details of the local moment-density potential used. The conventional Kohn–Sham potential $(\alpha\rho^{1/3})$ does not include these features adequately. The success of the self-consistent charge approximation to the molecular potential energy relies on the assumption that a sum of interpenetrating spherical charge distributions around each atomic center gives a good model for the total charge density of the molecule. The highly ionic lanthanide trihalides seem to be particularly favorable cases both for this model of molecular charge density and for the minimal optimized atomic basis set used here.

ACKNOWLEDGMENTS

It is a pleasure to acknowledge several useful discussions of the interpretation of these studies with Professor Don E. Ellis. We are grateful to have been able to build on the years of atomic and molecular calculational work that Professor Ellis and his co-workers have devoted to development of the discrete variational method.

Note added in proof: Additional electron diffraction studies on the structures of PrI_3, NdI_3, GdI_3, and LuI_3 [N. I. Popenko, E. Z. Zasorin, V. P. Spiridonov, and A. A. Ivanov, Inorg. Chim. Acta 31, L 371 (1978)] have been kindly called to our attention by Professor K. S. Krasnov. The Ln-X distances reported therein

differ from our estimates by ≤ 0.013 Å; such differences do not significantly alter the TSOE calculations reported here. However, the electron diffraction studies show that the above molecules are pyramidal, and we assumed planarity. Nevertheless, we have already noted in test cases (Sec. IV) that our calculations are not sufficiently sensitive to these geometry changes to alter our assignments and the quality of agreement with experiment, and hence do not affect the conclusions based on these calculations.

[1]J. Berkowitz, D. G. Streets, and A. Garritz, J. Chem. Phys. **70**, 1305 (1979).

[2]E. P. F. Lee, A. W. Potts, M. Doran, L. H. Hillier, J. J. Delaney, R. W. Hawksworth, and M. F. Guest, J. Chem. Soc. Faraday Trans. 2 **76**, 506 (1980).

[3]J. Berkowitz, C. H. Batson, and G. L. Goodman, J. Chem. Phys. **72**, 5829 (1980).

[4]A. W. Potts and E. P. F. Lee, Chem. Phys. Lett. **82**, 526 (1981).

[5]E. P. F. Lee, A. W. Potts, and J. E. Bloor, Proc. R. Soc. London Ser. A **381**, 373 (1982).

[6]J. Berkowitz, C. H. Batson, and G. L. Goodman, J. Chem. Phys. **71**, 2624 (1979).

[7]W. Carnall, P. Fields, and K. Rajnak, J. Chem. Phys. **49**, 4424 (1968).

[8]N. Beatham, P. A. Cox, A. F. Orchard, and I. P. Grant, Chem. Phys. Lett. **63**, 69 (1979).

[9]C. E. Myers, L. J. Norman II, and L. M. Loew, Inorg. Chem. **17**, 1581 (1978).

[10]P. Pyykkö and L. L. Lohr, Jr., Inorg. Chem. 20, 1950 (1981).

[11]C. F. Bender and E. R. Davidson, J. Inorg. Nucl. Chem. 42, 721 (1980).

[12]B. D. Snow, thesis, University of Tennessee, Knoxville, 1981.

[13]A. Rosen and D. E. Ellis, J. Chem. Phys. **62**, 3039 (1975); A. Rosen, D. E. Ellis, H. Adachi, and F. W. Averill, J. Chem. Phys. **65**, 3629 (1976).

[14]I. Lindgren and A. Rosén, Case Stud. At. Phys. **4**, 93 (1974); F. Herman and S. Skillman, *Atomic Structure Calculations* (Prentice–Hall, Englewood Cliffs, 1963).

[15]R. S. Mulliken, J. Chem. Phys. **23**, 1833, 1841 (1955).

[16]D. E. Ellis and G. L. Goodman, Int. J. Quantum Chem. (in press).

[17]B. Delley and D. E. Ellis, J. Chem. Phys. **76**, 1949 (1982).

[18]L. Hedin and B. I. Lundqvist, J. Phys. C **4**, 2064 (1971).

[19]U. von Barth and L. Hedin, J. Phys. C **5**, 1629 (1972).

[20]K. S. Krasnov, *Molekulyarn'ie Postoyann'ie Neorganicheskikh Soedinenii* (Khimiya, Leningrad, 1979),.

[21]G. Herzberg, *Molecular Spectra and Molecular Structure* III. *Electronic Spectra and Electronic Structure of Polyatomic Molecules* (Van Nostrand, Princeton, 1966).

[22]K. F. Zmbov and J. L. Margrave, in *Mass Spectrometry in Inorganic Chemistry*, Adv. Chem. Ser. No. 72 (American Chemical Society, Washington, D.C., 1968), p. 267; P. D. Kleinschmidt, K. H. Lau, and D. L. Hildenbrand, J. Chem. Phys. **74**, 653 (1981).

[23]G. K. Wertheim, in *Electron Spectroscopy: Theory Techniques and Applications*, edited by C. R. Brundle and A. D. Baker (Academic, London, 1978), Vol. 2, pp. 259–284.

[24]R. G. Egdell and A. F. Orchard, J. Chem. Soc. Faraday Trans. 2 **74**, 485 (1978).

[25]J. Berkowitz, in *Electron Spectroscopy: Theory, Techniques and Applications*, edited by C. R. Brundle and A. D. Baker (Academic, London, 1977), p. 355.

[26]L. L. Ames, P. N. Walsh, and D. White, J. Phys. Chem. **71**, 2707 (1967); E. Murad and D. L. Hildenbrand, J. Chem. Phys. **73**, 4005 (1980).

[27]J. W. Hastie, P. Ficalora, and J. L. Margrave, J. Less-Common Metals **14**, 83 (1968); S. Ciach, A. J. C. Nicholson, D. L. Swingler, and P. J. Thistlethwaite, Inorg. Chem. **12**, 2072 (1973).

[28]G. P. Dudchik, O. G. Polyachenok, and G. I. Novikov, Russ. J. Phys. Chem. **45**, 409 (1971).

[29]D. E. Work and H. A. Eick, High Temp. Sci. **5**, 313 (1973).

[30]C. Hirayama and P. M. Castle, J. Phys. Chem. **77**, 3110 (1973); C. Hirayama, G. L. Carlson, P. M. Castle, J. F. Rome, and W. E. Snider, J. Less-Common Metals **45**, 293 (1976).

[31]C. Hirayama, P. M. Castle, R. W. Liebermann, R. J. Zollweg, and F. E. Camp, Inorg. Chem. **13**, 2804 (1974).

[32]I. Hargittai, in *Topics in Current Chemistry*, (Springer, Berlin, 1981), Vol. 96, p. 43.

[33]W. C. Martin, R. Zalubas, and L. Hagan, *Atomic Energy Levels—The Rare-Earth Elements*, NSRDS-NBS 60 (National Bureau of Standards, Washington, D. C., 1978).

[34]A. V. Hariharan and H. A. Eick, High Temp. Sci. **4**, 379 (1972).